Food Hydrocolloids 160 (2025) 110792

Contents lists available at ScienceDirect

Food Hydrocolloids

journal homepage: www.elsevier.com/locate/foodhyd

Role of pulse globulins and albumins in air-water interface and foam stabilization

Penghui Shen [a], Solange M.L. Ha [a,b], Jinfeng Peng [c], Jasper Landman [a], Leonard M.C. Sagis [a,*]

[a] Laboratory of Physics and Physical Chemistry of Foods, Wageningen University, Bornse Weilanden 9, 6708 WG, Wageningen, the Netherlands
[b] Laboratory of Food Process Engineering, Wageningen University, Bornse Weilanden 9, 6708 WG, Wageningen, the Netherlands
[c] Danone Nutricia Global Research & Innovation Center, Utrecht, the Netherlands

ARTICLE INFO

Keywords:
Pulse protein
Air-water interface
Interfacial adsorption
Interfacial dilatational rheology
Interfacial structure
Foam
Correlation analysis

ABSTRACT

Pulse protein isolates are promising substitutes for animal protein in foam preparation, but they typically are complex mixtures of multiple proteins, and the contribution of the individual proteins to the behavior of the mixture in air-water interface stabilization is largely unknown. The major protein fractions in isolates are the globulins and albumins, and this study systematically investigated the molecular properties, and interfacial and foaming properties of these two fractions for three different pulses: lentils, faba beans and chickpeas. The key parameters of these pulse proteins in air-water interface and foam stabilization were investigated by correlation analysis. Based on this, low denaturation enthalpy tends to result in both high foamability and foam stability, most likely due to a greater conformational flexibility that allows for a faster adsorption to the air-water interface, and higher degree of structural rearrangement at the interface, which increases interfacial network stiffness. For globulin-rich pulse protein fractions, vicilins and convicilins tend to introduce high surface hydrophobicity, which increases the affinity of the proteins for the interface, and increases protein-protein in-plane interactions through hydrophobic interactions, resulting in the enhancement of interfacial network connectivity and the level of network branching. These factors increase the interfacial resistance to large deformations and increase foam stability. Vicilins and convicilins also tend to have a high value of the surface charge and further promote foam stability by increasing electrostatic repulsion between air bubbles. Legumins tend to reduce foamability since they adsorb to the air-water interface slowly and tend to disrupt the interfacial network structure. These findings provide deeper insights in the role of pulse globulins and albumins in air-water interface and foam stabilization. The proposed key parameters will benefit the predictability of the interfacial and foaming behavior of pulse proteins.

1. Introduction

Foam is one of the most common and important food systems. Common foam-based food products include milk foam, cream, cake, bread, mousse and meringue. In the food industry, foam is generally created with animal-based proteins such as whey protein, egg white protein and gelatin (Baziwane & He, 2003; Murray, 2020; Nasrollahzadeh, Nezafat, & Shafiei, 2021). The heavy dependence of the food industry on animal-based proteins is not sustainable due to the high consumption of land, water and energy, and the generated environmental problems like high greenhouse gas emissions, associated with the production of animal protein (Flachowsky, Meyer, & Südekum, 2018; Poore & Nemecek, 2018; Wu, Bazer, & Cross, 2014). Thus, animal protein alternatives are required, and plant proteins have been an important focus of attention (Chandran, Suri, & Choudhary, 2023; McClements & Grossmann, 2021; Mistry et al., 2022). Of the numerous types of plant protein resources that have been studied, pulse proteins are promising candidates for replacing animal proteins (K. K. Ma et al., 2022; Vogelsang-O'Dwyer, Zannini, & Arendt, 2021). Pulses are globally cultivated with 700–800 genera and around 19,000 systematized species. They are highly productive with a total worldwide production of more than 92 million tons in 2018 (Kumar & Pandey, 2020). The production of pulses is low cost and has positive environmental impacts, such as reduction of greenhouse emissions, water conservation and soil protection (Adarsh, Jacob, & Giffy, 2019; Khiangte & Siddique, 2021; Snyder, Bruulsema, Jensen, & Fixen, 2009). Moreover, pulses are rich in

* Corresponding author.
E-mail address: leonard.sagis@wur.nl (L.M.C. Sagis).

https://doi.org/10.1016/j.foodhyd.2024.110792
Received 5 August 2024; Received in revised form 1 October 2024; Accepted 28 October 2024
Available online 29 October 2024

proteins (19–40%) (Boukid, Zannini, Carini, & Vittadini, 2019; Raikos, Neacsu, Russell, & Duthie, 2014), and these proteins can be highly functional (e.g. foaming) for food industry applications (Hall & Moraru, 2021; Jarpa-Parra et al., 2017; Sharif et al., 2018; Shrestha, van 't Hag, Haritos, & Dhital, 2023).

Pulse proteins are complex mixtures mainly consisting of globulins (70–80%) and albumins (10–20%) (Shevkani, Singh, Chen, Kaur, & Yu, 2019). The globulins comprise legumins, vicilins and convicilins. The legumin globulins are hexamers with molecular weights of 300–400 kDa (Shevkani et al., 2019). Each legumin monomer contains one acidic polypeptide chain (~40 kDa) and one basic polypeptide chain (~20 kDa), and they are linked together by disulfide bonds (Shevkani et al., 2019). The vicilin globulins are trimers with molecular weights of 145–190 kDa, and consist of identical or heterogeneous polypeptide subunits formed by proteolysis during post-translational modification in seeds, and they lack cysteine (Krishnan & Coe, 2001; Shevkani et al., 2019). The convicilin globulins are trimeric globulin proteins with high homology with vicilins (González-Pérez & Arellano, 2009; Shevkani et al., 2019). They have molecular weights of 220–290 kDa and consists of 3–4 subunits that have molecular weight of around 70 kDa (Alfieri, Ververis, Precup, Julio-Gonzalez, & Noriega Fernández, 2023; Shevkani et al., 2019). Generally, convicilins exist in small amounts (González-Pérez et al., 2009; Shevkani et al., 2019). As for albumins, they are complex mixtures of enzymes, functional cytoplasmic proteins and storage proteins with broad molecular weight distributions (Emre, Turgut-balık, Genç, & Şahin, 2015; Shevkani et al., 2019; Varasundharosoth & Barnes, 1985; Švachulova, Turkova, & Klozová, 1982).

As clearly demonstrated, the protein components in pulses are different from each other in structure, which would cause different behavior in the stabilization of air-water interface and foam as already observed for globulins and albumins from rapeseed, Bambara groundnut, pea and mung bean (Shen, Yang, Nikiforidis, Mocking-Bode, & Sagis, 2023; Yang, de Wit et al., 2022; Yang, Kornet, et al., 2022). How the main protein components of pulses stabilize air-water interfaces and foam is still poorly understood, while that knowledge is essential for the valorization of pulse proteins in foam-based food product development.

In a previous study, we investigated the air-water interfacial and foaming properties of the full protein extracts from three mainstream pulses: lentil, faba bean and chickpea (Shen, Peng, Sagis, & Landman, 2024b). These pulse proteins were extracted in one-pot in alkaline conditions and had protein purities of 67–85 wt% and solubilities of 83–91%, and consisted mainly of globulins (68–81 wt%) with different vicilin and legumin contents, and a smaller fraction of albumins (19–32 wt%). All pulse protein extracts formed disordered viscoelastic solid-like interfaces at the air-water interface. The interface stabilized by lentil protein appeared to be comprised of globular proteins, similar to that stabilized by faba bean protein, but the lentil protein-stabilized interface had higher density, higher connectivity, longer protein threads, finer structures and higher stiffness than the faba bean protein-stabilized interface. The interface stabilized by chickpea protein appeared to be comprised of partially unfolded protein, and exhibited lower stiffness than the lentil protein-stabilized interface. Finally, lentil protein displayed higher foam half-life time than faba bean and chickpea proteins. It remains an open question how the observed differences in interfacial structure are related to the details of the protein molecular structure, and how the different protein components in pulse protein isolates contribute to their interfacial and foaming properties.

In this study, we further separated globulins and albumins from protein extracts of lentil, faba bean and chickpea, and investigated their individual roles in stabilizing air-water interfaces and foam. We comprehensively characterized their molecular properties such as protein composition, particle size, surface charge, surface hydrophobicity and thermal stability. We systematically measured their behavior at air-water interfaces, including interfacial adsorption kinetics on both short-time and long-time scales, and interfacial dilatational rheology in both the linear and non-linear response regimes, where the latter was analyzed with the general stress decomposition method (de Groot, Yang, & Sagis, 2023). We further studied their interfacial structures by imaging Langmuir-Blodgett films with atomic force microscopy (AFM) and measuring the interfacial thickness with ellipsometry. Those images were further subjected to image analysis to extract the characteristic protein domain size and network structure characteristics. Finally, we evaluated the foamability and foam stability of those pulse globulins and albumins. We performed correlation analysis on their molecular, interfacial and foaming properties to find out the key molecular and interfacial parameters that influence the foaming properties of those pulse proteins the most. This study is expected to provide deeper insights on the air-water interfacial behavior and foam stabilization properties of pulse proteins, which can help to screen for pulse proteins with high foaming performance and improve their functionalities. The proposed key parameters might be helpful in modelling studies on pulse proteins for the prediction of their interfacial and foaming behavior.

2. Materials and methods

2.1. Materials

Dehulled and split red lentil and faba bean, and whole chickpea were purchased from local pulse suppliers. All chemicals (Sigma-Aldrich, USA) were used as received. Ultrapure water (MilliQ Purelab Ultra, Germany) was used for all experiments unless stated otherwise.

2.2. Methods

2.2.1. Isolation of pulse globulins and albumins

Pulse globulins and albumins are separated using the classical alkaline extraction-acid precipitation method. All pulses were first milled into fine flours with a Hosokawa Multimill (Hosokawa Alpine, Augsburg, Germany) that was equipped with a UPZ fine impact mill. The flours were then mixed with water at 1:10 (w/w) ratio and magnetically stirred for 1 h, and the pH was kept at 8 using 1 M NaOH. Afterwards, the insoluble materials were removed by centrifugation at 20 °C. To achieve sufficient separation, the centrifugation duration and speed used were 20 min at 17,000 g for lentil, 15 min at 8000 g for faba bean and 60 min at 17,000 g for chickpea, respectively. After centrifugation, a supernatant and pellet layer appeared for lentil and faba bean flour suspensions, while another cream layer occurred in chickpea flour suspension due to the relatively abundant lipids in chickpea (Shen et al., 2024b). All supernatant layers were collected and adjusted to pH4.5 with 1 M HCl for 30 min, followed by centrifugation (17,000 g, 20 min, 20 °C) to obtain the albumin-rich supernatants and the globulin-rich pellets. Pellets were washed thrice with water, and centrifugation (17,000 g, 5 min, 20 °C) was applied every time after a wash. The washed pellets were then mixed with water at 1:6 (w/w) ratio and adjusted to pH7 with 1 M NaOH to redissolve the pellets. Finally, albumin-rich supernatants and globulin-rich dispersions were dialyzed against water using dialysis tubes with 3.5 kDa and 12–14 kDa cut-offs, respectively. This process lasted for two days with three times of water exchange, followed by freeze-drying. The freeze-dried samples were stored at 4 °C until further use.

2.2.2. Proximate analysis

The proximate analysis was performed according to our previous study (Shen, Peng, Sagis, & Landman, 2024a). In brief, protein content was measured using a Flash EA 1112 Series Dumas (Interscience, The Netherlands) with a nitrogen-to-protein conversion factor of 5.7. Total starch content was measured using an enzyme starch kit (Megazyme Inc., Ireland). Phenol content was measured with a Folin-Ciocalteu assay. Oil content was measured by Soxhlet extraction using a Soxtherm Unit Sox416 (C. Gerhardt, Königswinter, Germany). Water content was measured by determining the weight loss of samples after heating at 105 °C for 24 h. Ash content was measured in an ashing

furnace (Carbolite Gero, Germany) at 550 °C for 24 h. All measurements were conducted in at least duplicate.

2.2.3. Protein solubility

Samples were first dissolved in phosphate buffer (pH7.0, 20 mM) at 1% (w/w) extract concentration overnight and then filtrated over 0.22 μm syringe filters. The protein contents of the filtrates were determined with the Dumas method as mentioned above and used to calculate the protein solubility. The measurement was performed in triplicate.

2.2.4. Protein dispersion preparation

All protein samples for following measurements were prepared at 0.1% (w/w) soluble protein concentration in phosphate buffer (pH7.0, 20 mM) overnight, and were used after filtration through 0.22 μm syringe filters to remove all insoluble materials.

2.2.5. Physicochemical properties of pulse globulins and albumins

2.2.5.1. Protein composition. Protein composition of all protein extracts were measured using size exclusion chromatography (SEC) according to our previous study (Shen et al., 2024a). In brief, protein samples at 1% (w/w) extract concentration were eluted with phosphate buffer (pH7.0, 20 mM, containing 150 mM NaCl) in a Superdex 200 increase 10/300 GL column (Merck, Schnelldorf, Germany) on an Akta Pure 25 chromatography system (GE Healthcare, Diegem, Belgium). The flow rate was 0.75 mL/min. Protein was detected at a wavelength of 214 nm. Blue dextran (2000 kDa), ferritin (440 kDa), aldolase (158 kDa), conalbumin (75 kDa), ovalbumin (44 kDa), carbonic anhydrase (29 kDa), ribonuclease A (13.7 kDa), and aprotin (6.5 kDa) were measured as standards to determine the molecular weights of protein samples.

2.2.5.2. Particle size and surface charge. Protein particle size and surface charge were measured by dynamic light scattering and microelectrophoresis, respectively, on a Zetasizer (Nano ZS, Malvern Instruments, UK) at an extract concentration of 0.1% (w/w) in phosphate buffer (pH7.0, 20 mM). The refractive index was set as 1.450 for protein and 1.330 for water. All measurements were performed at 20 °C in triplicate.

2.2.5.3. Surface hydrophobicity. Surface hydrophobicity was measured according to our previous study (Shen et al., 2024b). Briefly, a fluorescence probe 8-anilino-1-napthalenesulfonic acid ammonium salt (ANSA) was applied and mixed with protein dispersions at protein concentration of 0–0.03% (w/w) for 1 h in the dark. The fluorescence intensities of the mixtures were measured at an excitation wavelength of 390 nm and an emission wavelength of 470 nm on an LS 50B luminescence spectrometer (PerkinElmer, USA). The slope of the linear regression of the fluorescence intensity as a function of protein concentration was taken as the surface hydrophobicity of a protein sample. The measurements were performed in at least duplicate.

2.2.6. Thermal stability

The thermal stabilities of protein extracts were evaluated by differential scanning calorimetry (DSC) on a Discovery DSC25 (TA Instruments, USA) according to our previous study (Shen et al., 2024b). Briefly, the temperature of protein samples at 10% (w/w) extract concentration was ramped from 20 to 140 °C at 5 °C/min in a stainless-steel high-volume pan sealed with a lid (TA Instruments, USA). The denaturation temperature and enthalpy were calculated by the TA Trios software. All measurements were performed in at least duplicate.

2.2.7. Protein adsorption kinetics at air-water interfaces

The adsorption kinetics of protein samples at air-water interfaces were measured based on our previous study (Shen et al., 2024a) on both the short-time scale and long-time scale. Briefly, a bubble pressure tensiometer (BPT) (BPT mobile, Krüss GmbH, Hamburg, Germany) was used for the short-time scale (10 ms–10 s) measurement. In this device, air bubbles were consecutively generated at a capillary tip (SH2510) into a protein dispersion (0.1%, w/w), and the pressure within the air bubbles was recorded and converted to surface tension by the built-in software. For the long-time scale measurement (1 s–3 h), an automated drop tensiometer (ADT) (Tracker, Teclis, Longessaigne, France) was applied. In the ADT, a rising bubble with area of 12 mm^2 was generated at the tip of a curved needle, and its shape was captured by a CCD camera system and fitted with the Young-Laplace equation to calculate the surface tension by the built-in software. Surface pressure was calculated by subtracting the surface tension of the samples from the surface tension of the clean air-water interface. All measurements were performed at room temperature (around 20 °C) in at least triplicate.

2.2.8. Interfacial dilatational rheology

Interfacial dilatational rheology was applied either continuously over a 5 h period (i.e., during adsorption), or after 3 h of equilibration, according to our previous study (Shen et al., 2024b). For the dilatational rheology performed during adsorption, sinusoidal oscillatory deformation was applied at an amplitude of 3% and a frequency of 0.02 Hz. For the experiments performed after 3 h of equilibration, frequency sweeps (0.0067–0.067 Hz, at an amplitude of 3%) or amplitude sweeps (2–50% amplitude, at a frequency of 0.02 Hz) were applied. The interfacial elastic modulus (E_d') and viscous modulus (E_d'') were calculated by Fourier transformation, using the built-in software. We also constructed Lissajous plots of surface pressure (the surface tension during oscillation minus the surface tension after 3 h of adsorption) versus intracycle strain ($=(A(t)-A_0)/A_0$); A_0 is the surface area in an undeformed state). The obtained Lissajous plots were further decomposed by the general stress decomposition (GSD) method established by (de Groot et al., 2023). All measurements were performed in at least triplicate at 20 °C.

2.2.9. Langmuir-Blodgett films

Langmuir-Blodgett (LB) films were prepared according to our previous study (Shen et al., 2024a). In short, protein samples were injected into a Langmuir trough (KSV NIMA/Biolin Scientific Oy, Finland) filled with phosphate buffer (pH7.0, 20 mM) and immersed with a freshly cleaved mica sheet (Highest Grade V1 Mica, Ted Pella, USA). Proteins were allowed to adsorb to the air-water interface for 3 h at room temperature (around 20 °C), and the surface pressure was monitored with a Wilhelmy plate. At the end of adsorption, the interface was compressed with two barriers at a speed of 5 mm/min. After the targeted surface pressure was reached, the mica was lifted at a speed of 1 mm/min. The prepared LB films were dried in a desiccator for at least two days.

2.2.10. Interfacial imaging

The LB films were imaged with atomic force microscopy (AFM) (NanoWizard® 4XP, NanoScience, Bruker Nano GmbH, Germany) based on our previous study (Shen et al., 2024a). Briefly, the films were scanned in a PeakForce Tapping® mode using a PEAKFORCE-HIRS-F-A cantilever (Bruker Nano GmbH, Germany). For each film, at least four images were captured over a 2×2 μm^2 or 350×350 nm^2 area, in a lateral resolution of 512 x 512 $pixels^2$. The images were further processed using the built-in JPK data processing software (Bruker Nano GmbH, Germany).

2.2.11. Image analysis

The AFM images were subjected to image analysis with *ImageJ* and *AngioTool 64* (National cancer Institute, National Institute of Health, Maryland, USA) according to our previous study (Shen et al., 2024a). In short, in *imageJ*, the pair correlation function (g(r)) macro was applied on the images after conversion into 8-bit grayscale, producing a curve of g(r) as a function of distance r from a reference point. After the curve was smoothed (with the Savitzky-Golay method), the r where g(r) decreases to 1 or to the first minimum (indicated by the first derivative curve of the smoothed g(r) curve) was taken as the protein domain size.

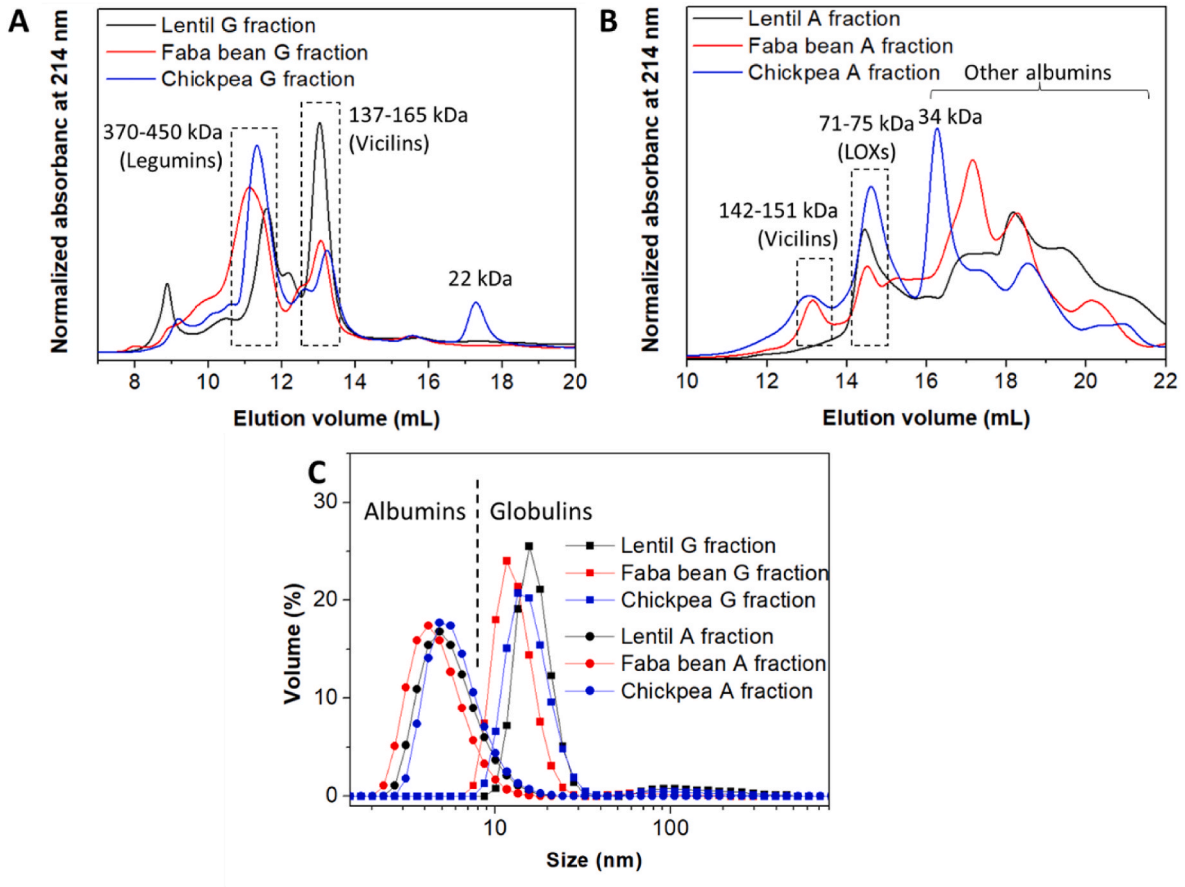

Fig. 1. Size exclusion chromatography (SEC) of globulin fractions (A) and albumin fractions (B) from lentil, faba bean and chickpea in phosphate buffer (20 mM, pH7) containing 150 mM NaCl measured at the wavelength of 214 nm. (C) Particle size distribution of those proteins in phosphate buffer (20 mM, pH7.0) after filtration over 0.22 μm filters. A representative particle size distribution was displayed from three replicates.

The maximum value of g(r) was used to indicate the heterogeneity of the distribution of interfacial structure. In *AngioTool 64*, the interfacial structure was selected and analyzed, producing a series of network parameters including vessel area, junction density, average vessel length and lacunarity. The vessel area indicates the area occupied by the protein network structure. The junction density describes the number of junctions formed by protein threads in a unit area of the whole protein network. The average vessel length indicates the average length of protein threads. The lacunarity indicates the heterogeneity of the distribution of voids within structures, and lower lacunarity implies lower heterogeneity of the structures. The branching rate was calculated from the total number of junctions divided by vessel area, and the end-point rate was calculated from the total number of end points divided by vessel area (Shen et al., 2024b).

2.2.12. Foaming properties

2.2.12.1. Foam overrun. Foam overrun of pulse proteins was measured by whipping 15 mL of protein dispersion (0.1% w/w) at 2000 rpm for 2 min with a frother (Aerolatte, UK) in a cylindrical plastic tube (diameter of 34 mm). The height of the foam was immediately marked after whipping. The volume of generated foam divided by 15 mL (and multiplied by 100%) was taken as the foam overrun. Foams were prepared in at least triplicate at room temperature (around 20 °C).

2.2.12.2. Foam half-life time. The generated foam by whipping was quickly transferred to a 50 mL gradient cylinder using a spoon. The cylinder was covered with a film to avoid water evaporation. The time when half of the foam decayed was taken as the foam half-life time. The measurements were performed in at least triplicate at room temperature (around 20 °C).

2.2.13. Statistical analysis

One-way analysis of variance (ANOVA) of the data was performed with IBM SPSS Statistics 19. Duncan tests were used for comparison of mean values using a level of significance of 5%. Correlation analysis was performed with the same software, and one-tailed Pearson correlation tests were applied.

3. Results and discussion

3.1. Physicochemical properties of pulse globulins and albumins

3.1.1. Proximate composition

According to the proximate analysis (Table S1), the globulin fractions of lentil, faba bean and chickpea all have high protein purities with protein content of 88.6 (±0.7) wt%, 85.2 (±0.5) wt% and 79.7 (±0.3) wt %, respectively. The amount of impurities, including starch, ash, phenol and oil, are negligible. The albumin fractions have pronouncedly lower protein purity, which is 67.5 (±0.4) wt%, 59.7 (±0.4) wt% and 55.5 (±0.4) wt%, respectively, for lentil, faba bean and chickpea albumin fractions. These albumin fractions are slightly rich in starch (7–12 wt%), but poor in other impurities. Starches are generally large particles (0.5–100 μm) (Xu et al., 2020), and they are expected to be efficiently removed by membrane filtration with a small pore size (0.22 μm in this study). After the whole proximate analyses, 72–90 wt% of the compounds in albumin fractions were resolved, which is lower than for the globulin fractions (90–100 wt%). The unresolved impurities are likely to

Table 1
Molecular properties of the globulin and albumin fractions from lentil, faba bean and chickpea. The contents of globulins, legumin, vicilin and convicilin, and albumins were calculated based on size exclusion chromatograms. Thermal properties of proteins were measured using differential scanning calorimetry (DSC). The averages and standard deviations were the results of at least two replicates.

	Globulin fractions			Albumin fractions		
	Lentil	Faba bean	Chickpea	Lentil	Faba bean	Chickpea
Content of globulins (%)	82.3	74.3	79.7	0	6.4	12.5
Legumins/(vicilins + convicilins) ratio	0.5	1.7	1.6	0	0	0
Content of legumins (%)	28.0	47.2	42.8	0	0	0
Content of vicilins + convicilins (%)	54.3	27.1	26.9	0	6.4	12.5
Content of albumins (%)	5.7	12.4	1.6	97.9	93.4	87.5
Zeta potential (mV)	−18 ± 1	−15 ± 1	−15 ± 1	−5 ± 2	−6 ± 3	−6 ± 4
Relative surface hydrophobicity	1.49 ± 0.02	0.64 ± 0.01	0.74 ± 0.05	0.25 ± 0.00	0.43 ± 0.00	0.94 ± 0.01
Onset temperature (°C)	71.8 ± 0.1	73.7 ± 0.5	74.5 ± 0.5	69.5 ± 0.4	72.5 ± 0.3	61.7 ± 0.7
Denaturation temperature at 1_{st} peak (°C)	83.0 ± 0.0	86.7 ± 0.3	77.7 ± 0.3	75.5 ± 0.2	76.9 ± 0.1	75.1 ± 0.4
Denaturation temperature at 2_{nd} peak (°C)	–	–	92.2 ± 0.1	84.6 ± 0.2	85.3 ± 0.7	92 ± 5
Total enthalpy (J/g protein)	8.3 ± 0.4	11.2 ± 0.4	13.0 ± 0.9	3.7 ± 0.5	0.61 ± 0.05	3.9 ± 0.2

be dietary fibers, which are abundant in pulses (20–25 wt%) (Chen, McGee, Vandemark, Brick, & Thompson, 2016; Dhull, Kidwai, Noor, Chawla, & Rose, 2022). The dietary fibers from pulses are highly hydrophilic (N. Wang & Toews, 2011) and are not expected to adsorb to the air-water interface. All globulin and albumin fractions have high protein solubilities, especially the albumin fractions, which are 94 (±1)%, 93.5 (±0.3)% and 98.8 (±1.1)%, respectively, for lentil, faba bean and chickpea albumins (Table S1). For lentil, faba bean and chickpea globulin fractions, their solubilities are 92 (±2)%, 84.5 (±0.5)% and 88.7 (±0.7)%, respectively.

3.1.2. Protein composition, particle size and surface charge

According to the size exclusion chromatograms of the globulin fractions (Fig. 1A), they mainly consist of legumin and vicilin globulins with total globulin content of 74.3–82.3% and small proportions of albumins (1.6–12.4%) (Table 1). The lentil globulin fraction is rich in vicilin and convicilin (54.3%), and faba bean and chickpea globulin fractions are rich in legumins (42.8–47.2%). All albumin fractions comprise various non-globulin proteins (87.5–97.9%) with rather broad molecular weight distributions (Fig. 1B), indicating the high heterogeneity in the protein compositions of albumin fractions, which include enzymes (e.g. lipoxygenase), functional cytoplasmic proteins and storage proteins (e.g. 2S albumins) (Emre et al., 2015; Shevkani et al., 2019; Švachulova et al., 1982; Varasundharosoth et al., 1985). There are no globulins in the lentil albumin fraction and small amounts of vicilin globulins (6.4–12.5%) in the faba bean and chickpea albumin fractions (Table 1). The particle size distributions of the globulin fractions display peaks around 10–15 nm (Fig. 1C), and their zeta potential is between −15.1 and −18.4 mV (Table 1). As for the albumin fractions, their particle size distributions have peaks around 4–5 nm (Fig. 1C), and their zeta potential is around −6 mV (Table 1).

3.1.3. Surface hydrophobicity

Surface hydrophobicity is widely accepted as an important molecular parameter influencing the interfacial behavior of proteins and their final functionalities (Shevkani et al., 2019; Tang, 2017; Wierenga & Gruppen, 2010). The lentil globulin fraction has about one-fold higher surface hydrophobicity than faba bean and chickpea globulin fractions, and also has a higher ratio of lentil vicilin and convicilin to legumin, compared to those of faba bean and chickpea globulin fractions (Table 1). This suggests that vicilins (likely together with convicilins) dominate the surface hydrophobicity of these pulse globulins, which has also been observed in Bambara groundnut proteins (Alabi, Ali, Nwachukwu, Aluko, & Amonsou, 2020). Cserhalmi, Czukor, and Gajzágó-Schuster (1998) studied the surface hydrophobicity of vicilin and legumin fractions from five pea varieties, and they found that in general, the vicilin fractions had higher surface hydrophobicity than legumin fractions. Compared to vicilin, legumin has a more rigid and compact structure, consisting of parallel hexagonal rings which would facilitate the maximal packing of its quaternary structure and in turn maximize its hydrophilicity (Tang, 2017). The hydrophobic basic polypeptides of legumin form the core of each subunit, surrounded by the more hydrophilic acidic polypeptides (Kuang, 2022; Shewry & Casey, 1999). However, some studies showed that legumins had higher surface hydrophobicity than vicilins (Sha & Xiong, 2022; Q. Shen, Yang, et al., 2023; Yang, de Wit et al., 2022), which might be caused by the protein extraction and purification process. For example, the Bambara groundnut protein extracted by isoelectric point precipitation displayed higher surface hydrophobicity than that without such a step (Yang, de Wit et al., 2022), where the pH shifting process might have caused the exposure of interior hydrophobic groups. Both lentil and faba bean albumin fractions display pronouncedly lower surface hydrophobicity than their corresponding globulin fractions (Table 1), which is commonly observed for albumins and globulins from the same source (Cserhalmi et al., 1998; Osemwota, Alashi, & Aluko, 2022; Ye et al., 2024). The chickpea albumin fraction shows higher surface hydrophobicity than the chickpea globulin fraction (Table 1), which could be due to the higher content of lipoxygenase in chickpea albumin (Fig. 1B) which has a hydrophobic channel for substrate accommodation (Newcomer & Brash, 2015) or due to other protein components (e.g. the most abundant one at 34 kDa (Fig. 1B). The exact reason warrants further studies. The high surface hydrophobicity of chickpea albumin fraction well explains the higher surface hydrophobicity of the whole chickpea protein extract compared to the whole lentil protein extract in our previous study (Shen et al., 2024b), where the whole chickpea protein had a higher albumin fraction although its globulin components display lower surface hydrophobicity than those of lentil (Table 1).

3.1.4. Thermal stability

The thermal stability of all protein fractions was evaluated with differential scanning calorimetry (DSC). All globulin fractions start to denature at temperatures between 71.8 and 74.5 °C (Table 1; Fig. S1), which is ascribed to the beginning of the denaturation of vicilins due to their more flexible structures and lower thermal stabilities than legumins (Gravel & Doyen, 2023; Tang, 2017). The lentil globulin fraction shows a main denaturation peak at 83 °C, lower than those of faba bean (86.7 °C) and chickpea globulin fractions (92.2 °C) (Table 1; Fig. S1). It also displays a lower denaturation enthalpy of 8.3 (±0.4) J/(g protein) compared to those of faba bean (11.2 ± 0.4 J/(g protein)) and chickpea globulin fractions (13.0 ± 0.9 J/(g protein)) (Table 1). These phenomena are attributed to the higher content of vicilins in the lentil globulin fraction than the other globulin fractions (Fig. 1A). All albumin fractions demonstrate lower denaturation temperatures (61.7–72.5 °C) than their corresponding globulin fractions, and they meanwhile have much lower denaturation enthalpies (0.61–3.9 J/(g protein)) (Table 1; Fig. S1), suggesting that these albumin fractions overall have much lower thermal stabilities than the globulin fractions. These phenomena could be partially derived from the high molecular flexibility of metabolic

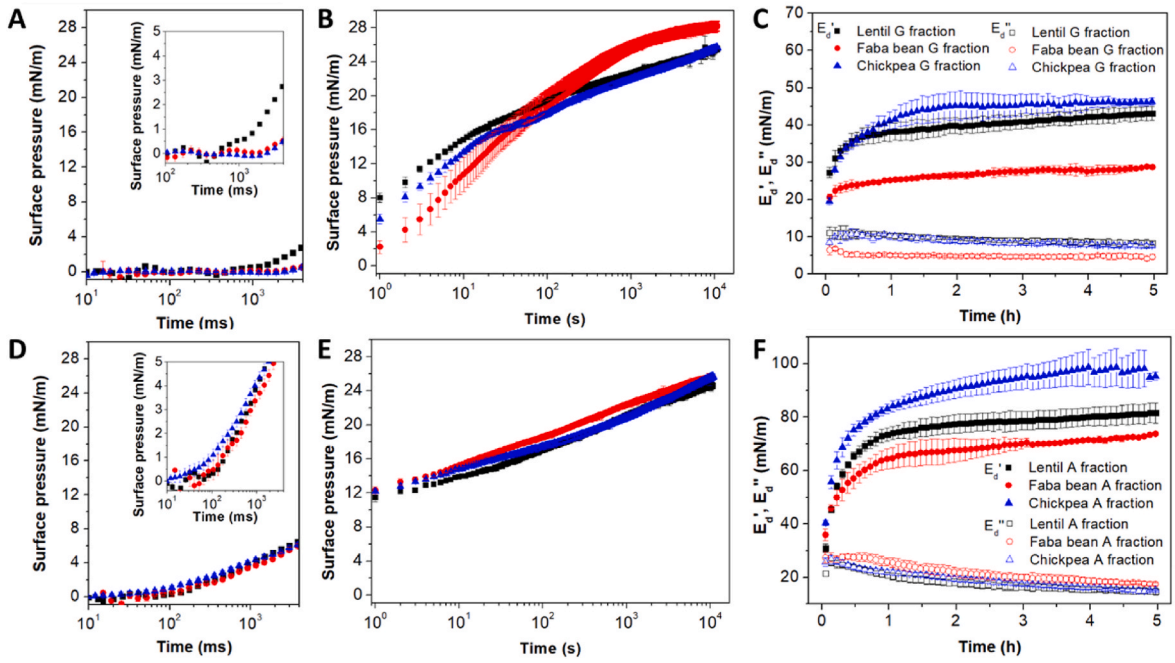

Fig. 2. Surface pressure of the globulin and albumin fractions from lentil, faba bean and chickpea as a function of time within the sub-second regime measured by bubble pressure tensiometer (BPI) (A, D) and long-time regime measured by automated drop tensiometer (ADT) (B, E), at the air-water interface at 20 °C. The inserts in Fig. A and D zoom in on the onset of the increase of surface pressure. (C, F) Dilatational elastic modulus (E_d') and viscous modulus (E_d'') of the interfaces formed by the globulin and albumin fractions from lentil, faba bean and chickpea proteins with adsorption time measured on the ADT at amplitude of 3% and frequency of 0.02 Hz. Protein dispersions containing 0.1% (w/w) soluble protein were prepared in phosphate buffer (20 mM, pH7) and filtrated through 0.22 μm filters. The averages and standard deviations were calculated from at least three replicates.

enzyme proteins in the albumin fractions (Kokkinidis, Glykos, & Fadouloglou, 2012).

3.2. Interfacial adsorption kinetics

The adsorption kinetics of lentil, faba bean and chickpea globulins and albumins at the air-water interfaces were measured on short-time scales (10 ms-4 s) using a bubble pressure tensiometer (BPT) and on long-time scales (1 s-3 h) using an automated drop tensiometer (ADT). In the short-time scale measurements, the adsorption induction time is 85, 50 and 19 ms for lentil, faba bean and chickpea albumin fractions, respectively (Fig. 2D), which is much shorter than their corresponding globulin fractions. The adsorption induction time is 600, 1900 and 1900 ms for lentil, faba bean and chickpea globulin fractions, respectively (Fig. 2A). Thus albumins clearly adsorb to air-water interfaces much faster than globulins due to their much smaller particle size (Fig. 1C) and lower surface charge values (Table 1) that can lead to higher diffusion rates towards the interface and a lower interfacial adsorption energy barrier. Within the albumin fractions, the chickpea albumin fraction adsorbs faster to the interface than the others, which is ascribed to its pronouncedly higher surface hydrophobicity (Table 1). Within the globulin fractions, the lentil globulin fraction adsorbs the fastest to air-water interface, and faba bean and chickpea globulins display comparably slower adsorption rates (Fig. 2A). From protein composition measurements, the lentil globulin fraction has the highest content of vicilin and convicilin, and faba bean and chickpea globulin fractions have comparably lower amount of those proteins (Table 1). In general, vicilins adsorb to interface faster than legumins due to their higher surface hydrophobicity, lower molecular weights and less rigid molecular structures (Dagorn-Scaviner, Gueguen, & Lefebvre, 1986; Tang, 2017). According to our previous study, the whole lentil, faba bean and chickpea protein extracts have induction times of 300, 450 and 360 ms, respectively, which are pronouncedly lower than that of corresponding globulin fractions. These whole pulse protein extracts contain only small amounts of albumins (17.6–25.5%), but the presence of these albumins in pulse proteins can markedly decrease their adsorption induction time, which was also observed in mixtures of rapeseed globulins and albumins (P. Shen, Yang, et al., 2023).

In the long-time scale measurements and in all protein samples, the surface pressure was still increasing after 3 h of adsorption (Fig. 2B–E) because of the slowly ongoing rearrangements of the microstructure formed by the proteins at the interface. These rearrangements are induced by thermal fluctuations, and due to crowding of the interface become increasingly stochastic. This results in slow increases in the surface pressure which can last for at least a few days (Mitropoulos, Mütze, & Fischer, 2014). Regarding the globulin fractions, lentil and chickpea display similar adsorption patterns and finally reached surface pressures of around 26 mN/m. The faba bean globulin fraction increased surface pressure at a faster rate in the first few hundreds of seconds and finally reached a higher surface pressure of 28.2 (±0.6) mN/m. As for the albumin fractions, they demonstrate rather similar adsorption patterns during the whole 3 h of adsorption, and they finally reached similar surface pressures around 25 mN/m.

During the interfacial adsorption, we also monitored the development of interfacial stiffness by applying small amplitude oscillatory dilatation on the air-water interfaces. The first data point was measured after 50 s of adsorption, where the elastic modulus (E_d') was already larger than the viscous modulus (E_d'') for all protein samples (Fig. 2C–F), indicating the fast formation of viscoelastic solid-like interfaces for both pulse globulin and albumin fractions, which agrees with the barely unchanged interfacial thickness during 3 h of adsorption (Fig. S4). For all protein samples, E_d' was increasing while E_d'' was decreasing (Fig. 2C–F), which implies the increase of interfacial stiffness and elasticity during the aging of the interface. The changes of E_d' and E_d'' almost reach a plateau after 3 h of adsorption (Fig. 2C–F), which suggests the interfaces have reached a quasi-equilibrium state at that point. Finally, albumin fractions display pronouncedly higher E_d' than all the globulin fractions (Fig. 2C–F), indicating that the albumin

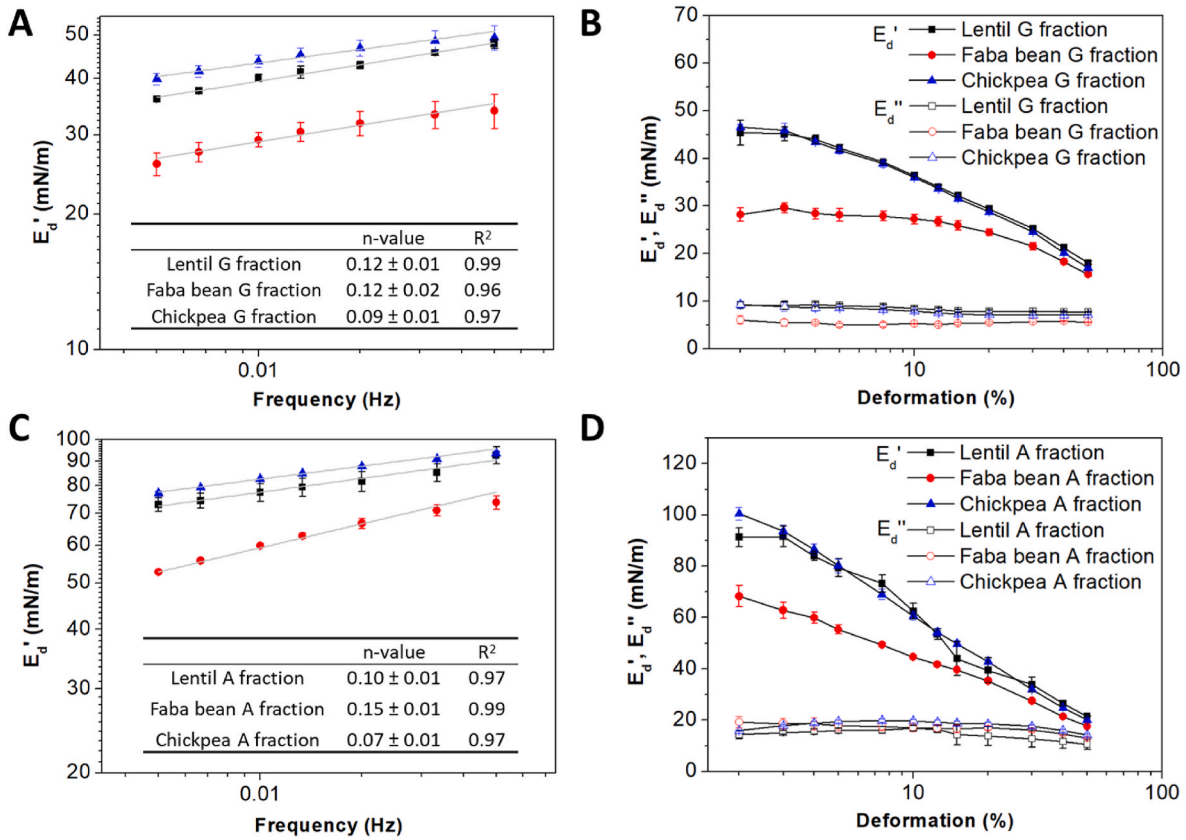

Fig. 3. Dilatational elastic modulus (E_d') and viscous modulus (E_d'') of the interfaces formed by the globulin and albumin fractions from lentil, faba bean and chickpea as a function of frequency at a fixed amplitude of 3% (A, C) or as a function of amplitude of deformation at a fixed frequency of 0.02 Hz (B, D) after 3 h of adsorption of proteins to the air-water interface at 20 °C. The solid lines in Fig. A and C for E_d' represent power-law fits (E_d'~ω^n) of the data points with insets summarizing the slopes (n-values) and the coefficients of determination. Protein dispersions containing 0.1% (w/w) soluble protein were prepared in phosphate buffer (20 mM, pH7) and filtered through 0.22 μm filters. The averages and standard deviations were the results of at least three replicates.

fractions formed stiffer interfaces. Within the albumin fractions, the chickpea albumin fraction has the highest E_d' of 95.3 (±1.4) mN/m, followed by the lentil albumin fraction (82 ± 4 mN/m) and the faba bean albumin fraction (73.8 ± 0.4 mN/m) (Fig. 2F). The highest E_d' of chickpea albumin fraction is probably due to its higher surface hydrophobicity (Table 1), where the hydrophobic patches of proteins can increase protein-protein in-plane interactions through hydrophobic interactions. The chickpea globulin fraction has slightly higher E_d' (46 ± 1 mN/m) than the lentil globulin fraction (43.1 ± 1.8 mN/m), while faba bean globulin has the lowest E_d' (28.7 ± 0.2 mN/m) (Fig. 2C). The E_d' of these globulin fractions are close to those of the whole protein extracts (36–50 mN/m) (Shen et al., 2024b), suggesting the dominance of globulins in the interfacial stiffness of the whole protein extracts because of their high contents.

During interfacial aging, the surface pressures and elastic moduli of all samples (except chickpea globulin fraction) start to follow either logarithmic or power-law behavior after adsorption for a certain time (Table S2; Fig. S2), which are typical aging features of disordered glass-like solids (Negi & Osuji, 2010; Shohat, Friedman, & Lahini, 2023). Overall, the surface pressure and elastic moduli of albumin fractions tend to have a somewhat higher rate of aging compared to the globulin fractions (Table S2), suggesting faster rearrangement of the interfacial structures formed by the albumin fractions, indicating a higher mobility at the interface, most likely due to their smaller size (Fig. 1C) and lower surface charge (Table 1).

3.3. Interfacial dilatational rheology

After 3 h of adsorption, the interfaces stabilized by globulin and albumin fractions were subjected to dilatational deformations in both frequency sweeps and amplitude sweeps. In the frequency sweeps (0.0067–0.067 Hz at a deformation amplitude of 3%), the moduli E_d' of all interfaces follow power-law behavior with frequency (E_d'~ω^n), and the values for the exponent n are between 0.07 and 0.15 (Fig. 3A–C), which are much lower than 0.5 and show a weak dependency on frequency. The n-value of 0.5 is predicted by the Lucassen & van den Tempel model (Lucassen & Van Den Tempel, 1972) and indicates the dominance of material exchange between bulk and interface in the response of the interface to dilatational deformation. Values for n much lower than 0.5 suggest low exchangeability of those globulin and albumin fractions after adsorption at the interface, and that the interfaces are in a disordered solid-like state with a wide spectrum of relaxation times. This was also observed for the whole pulse protein extracts (Shen et al., 2024b) and many other proteins (e.g. rapeseed proteins (P. Shen, Yang, et al., 2023), lupin proteins (X. Ma, Shen, Habibi, & Sagis, 2024), Bambara groundnut proteins (Yang, de Wit et al., 2022) and whey protein (Yang et al., 2021)).

In the amplitude sweeps (2–50% at a frequency of 0.02 Hz), E_d' values at 2% deformation amplitude (Fig. 3B–D) are comparable to the plateaus of E_d' measured during adsorption (Fig. 2C–F). With increasing deformation amplitudes, the moduli E_d' decrease but remain higher than E_d'' (Fig. 3B–D). This indicates the interfacial structures were increasingly disrupted but still retained solid-like characteristics. At deformation amplitude of 50%, E_d' of all interfaces decreases to 16–20 mN/m, where the E_d' of the albumin fractions decreases by much higher extents (71–78%) than those of the globulin fractions (37–59%) (Fig. 3B–D), suggesting more severe disruption of interfacial structures for the albumin fractions. The lentil and chickpea globulin fractions (Fig. 3B), and

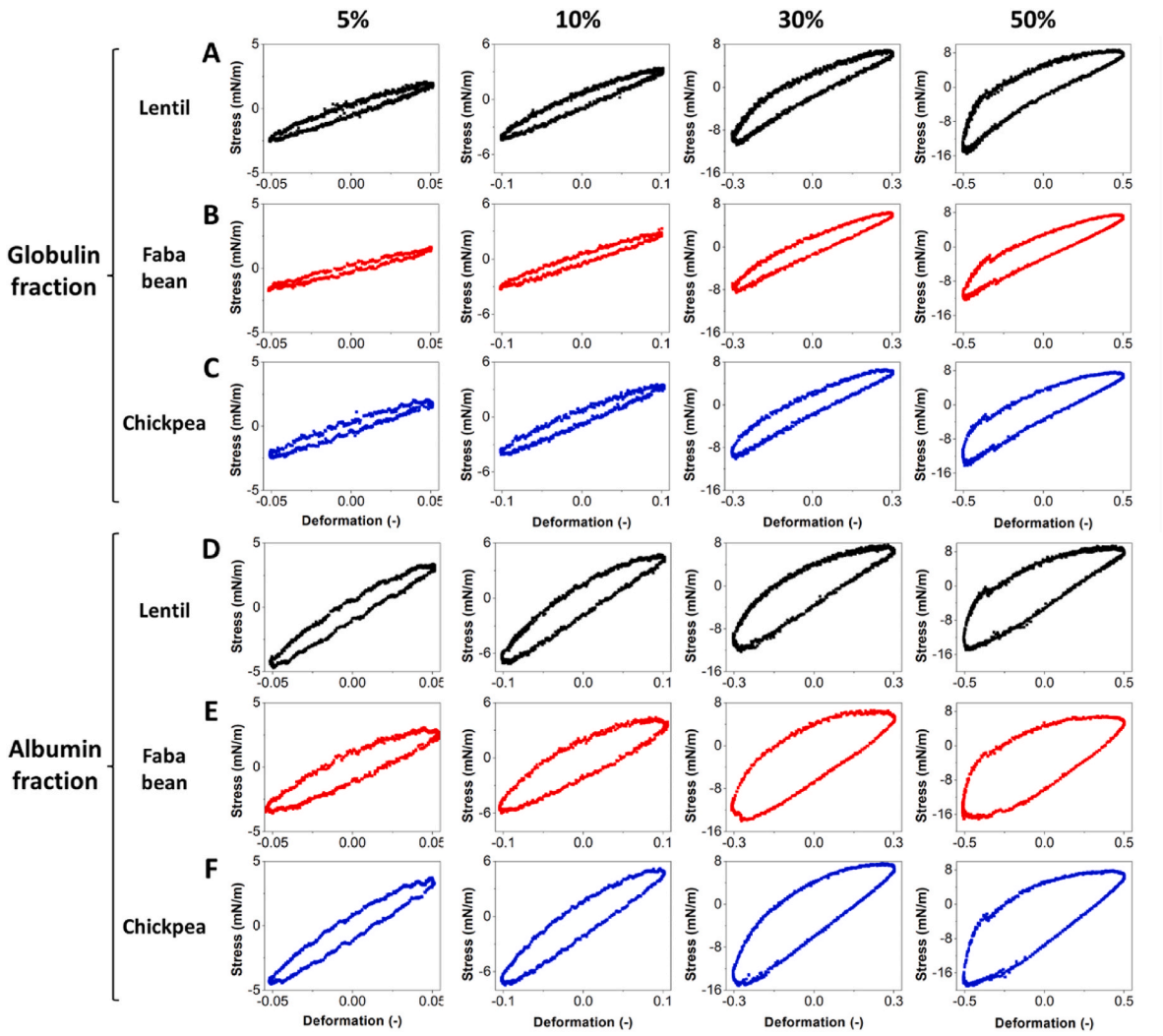

Fig. 4. Lissajous plots of the globulin and albumin fractions from lentil (A, D), faba bean (B, E) and chickpea (C, F) at amplitudes of 5%, 10%, 30% and 50% at a fixed frequency of 0.02 Hz. For clarity, one representative plot or curve was displayed for each condition from at least three replicates.

lentil and chickpea albumin fractions (Fig. 3D), display highly comparable decrease patterns of E_d', respectively.

In the calculation of E_d', only the intensity and phase of the first harmonic of the Fourier transform of the total surface stress was considered. In the non-linear regime, higher harmonics exist and have distinct contributions to the overall stress response to deformation, which are typically neglected. To comprehensively depict the rheological behavior of these proteins at air-water interfaces, Lissajous plots were constructed and analyzed in a quantitative way using the general stress decomposition method (de Groot et al., 2023), as described in the following section.

3.4. Lissajous plots and surface stress decomposition

3.4.1. Lissajous plots

Lissajous plots were plotted as surface stress (intracycle surface pressure) versus intracycle deformation. In Lissajous plots from interfacial dilatational rheology, the upper part describes interfacial expansion, and the lower part describes interfacial compression. Purely elastic interfaces generate a straight line in Lissajous plots, purely viscous interfaces generate circular Lissajous plots, and viscoelastic interfaces generate elliptic Lissajous plots (Sagis & Scholten, 2014). The occurrence of non-linear behavior will distort dilatational Lissajous plots to an asymmetric shape.

At a small deformation amplitude of 5%, the Lissajous plots of all globulin and albumin fractions are elliptic (Fig. 4), indicating linear viscoelastic behavior of all interfaces. The areas enclosed by the Lissajous plots of albumin fractions (Fig. 4D–F) are distinctly larger than those of globulin fractions (Fig. 4A–C), which suggests more significant viscous dissipation in interfaces stabilized by albumins. With the deformation amplitude increasing to 10%, the Lissajous plots of all globulin fractions are still basically linear (Fig. 4A–C), while those of the albumin fractions start to show nonlinear behavior with mild strain softening during surface expansion: the slope of the curve starts to level off to zero, towards maximum expansion (Fig. 4D–F). This behavior becomes clearer as the amplitude is increased to 30%. At 30% deformation amplitude, the Lissajous plots of the globulin fractions also start to display strain softening behavior (Fig. 4A–C), while their enclosed areas are still smaller than those of the albumin fractions (Fig. 4D–F). With the deformation amplitude further increasing to 50%, the Lissajous plots of all samples exhibit increased areas and strain softening behavior during surface expansion (Fig. 4), especially for the albumin fractions (Fig. 4D–F), suggesting significant effects of structure disruption and surface density changes for the albumin-stabilized interfaces. Within the globulin fractions (Fig. 4A–C), the Lissajous plots of lentil display a higher initial elastic response and thereafter more obvious strain softening during surface expansion, and more obvious strain hardening during surface compression. The latter is obvious from the increase in

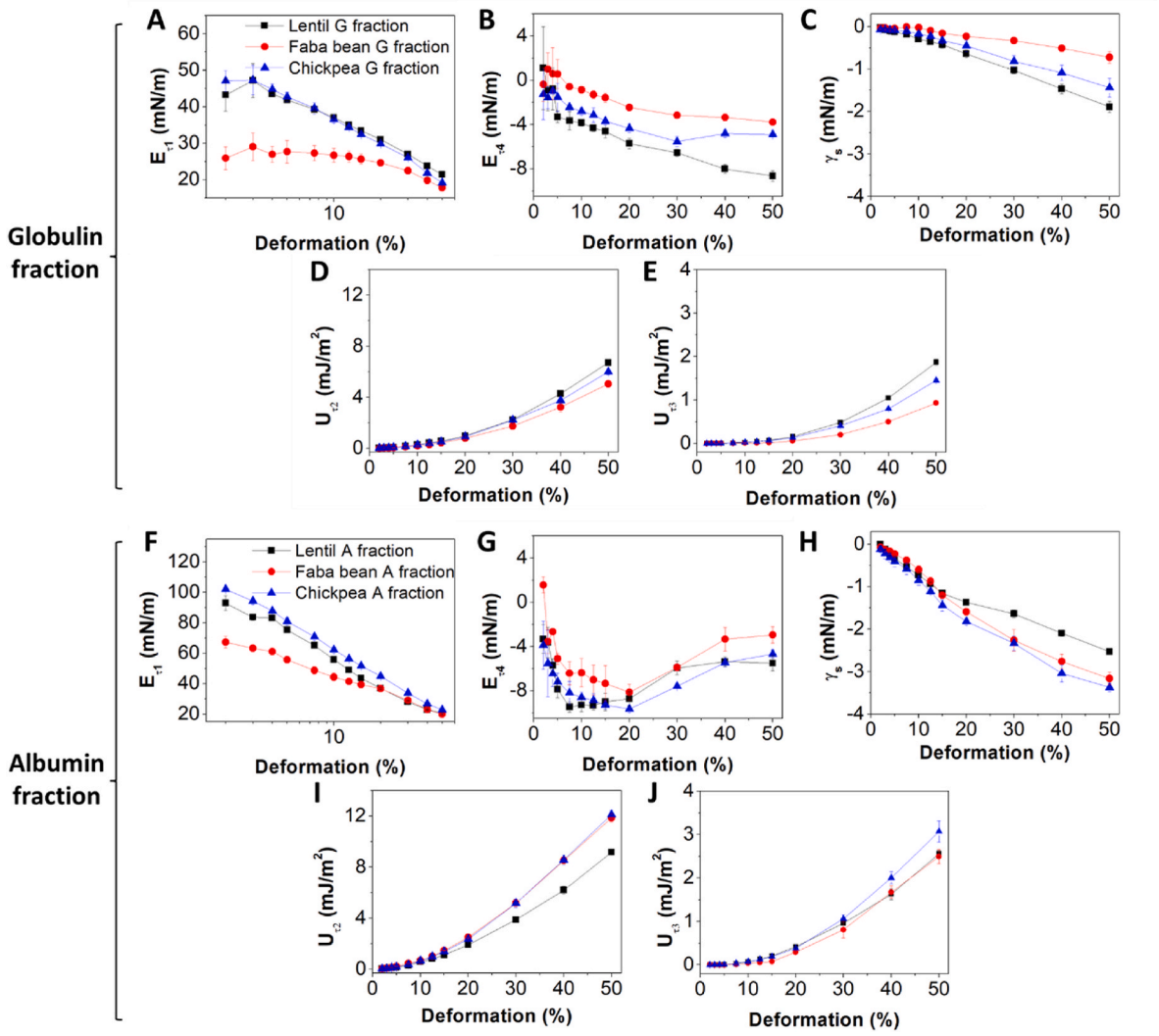

Fig. 5. Modulus of τ_1 ($E_{\tau1}$) (A,F) and τ_4 ($E_{\tau4}$) (B,G), and dissipated energy of τ_2 ($U_{\tau2}$) (D,I) and τ_3 ($U_{\tau3}$) (E,J) and vertical shift (γ_s) (C,H) of the globulin (A–E) and albumin fractions (F–J) from lentil, faba bean and chickpea as a function of amplitude deformation after stress decomposition. The averages and standard deviations were the results of at least three replicates.

slope of the curve towards maximum compression (the lower-left corner of the loop). This might reflect stronger in-plane interactions of lentil globulin at air-water interfaces than the other globulins (Yang, Thielen, Berton-Carabin, van der Linden, & Sagis, 2020), and is mostly ascribed to a higher extent of jamming of the interfacial structures (Yang et al., 2020), which also occurred more pronouncedly for the lentil whole protein extract compared to faba bean and chickpea whole protein extracts (Shen et al., 2024b).

3.4.2. *General stress decomposition of Lissajous plots*

From the asymmetry of the Lissajous plots at high deformation amplitudes, we can already see that changes in both interfacial structure and surface density play a role in the surface stress responses to interfacial dilatational deformation. To split the contributions from those two factors, the general stress decomposition method (de Groot et al., 2023) was applied. The total stress was split into four components: τ_1, τ_2, τ_3 and τ_4. Here, τ_1 and τ_2 are the elastic and viscous components, respectively, together describing the contributions from odd harmonics to the total stress. Then, τ_3 and τ_4 are the viscous and elastic components, respectively, together describing the contributions from even harmonics to the total stress. The higher odd harmonics represent the nonlinear contributions to the surface stress induced by changes in the interfacial network structure, and the even harmonics represent the contributions from interfacial density change (de Groot et al., 2023). From quantitative analysis on the decomposed stresses, five parameters were produced including $E_{\tau1}$, $U_{\tau2}$, $U_{\tau3}$, $E_{\tau4}$, and γ_s. $E_{\tau1}$ and $E_{\tau4}$ are two secant elastic moduli, describing the interfacial network stiffness and resistance to interfacial density change, respectively. $U_{\tau2}$ and $U_{\tau3}$ are two dissipated energies per unit area, from interfacial structure disruption and interfacial density change, respectively. Furthermore, γ_s measures the baseline shift of the oscillation with respect to the initial quasi-equilibrium state, and is a measure how far the oscillations drive the interface out of equilibrium.

For all samples, the values for $E_{\tau1}$ are significantly larger than $E_{\tau4}$ values over the entire strain range (Fig. 5A,B,F,G), and similarly $U_{\tau2}$ values are larger than $U_{\tau3}$ (Fig. 5D,E,I,J), suggesting that the contributions to the stress response from interfacial network changes are more important than those from interfacial density changes, and the interfacial stiffness mainly comes from the generated interfacial network structure. At a deformation amplitude of 2%, the moduli $E_{\tau1}$ of albumin-stabilized interfaces (Fig. 5F) are considerably higher than those of globulin-stabilized interfaces (Fig. 5A), indicating that the albumin fractions formed much stiffer interfacial network structures than the globulin fractions. Interestingly, the chickpea and lentil albumin fractions have comparable interfacial network stiffness, and so do the globulins of these two sources, but chickpea whole protein extract

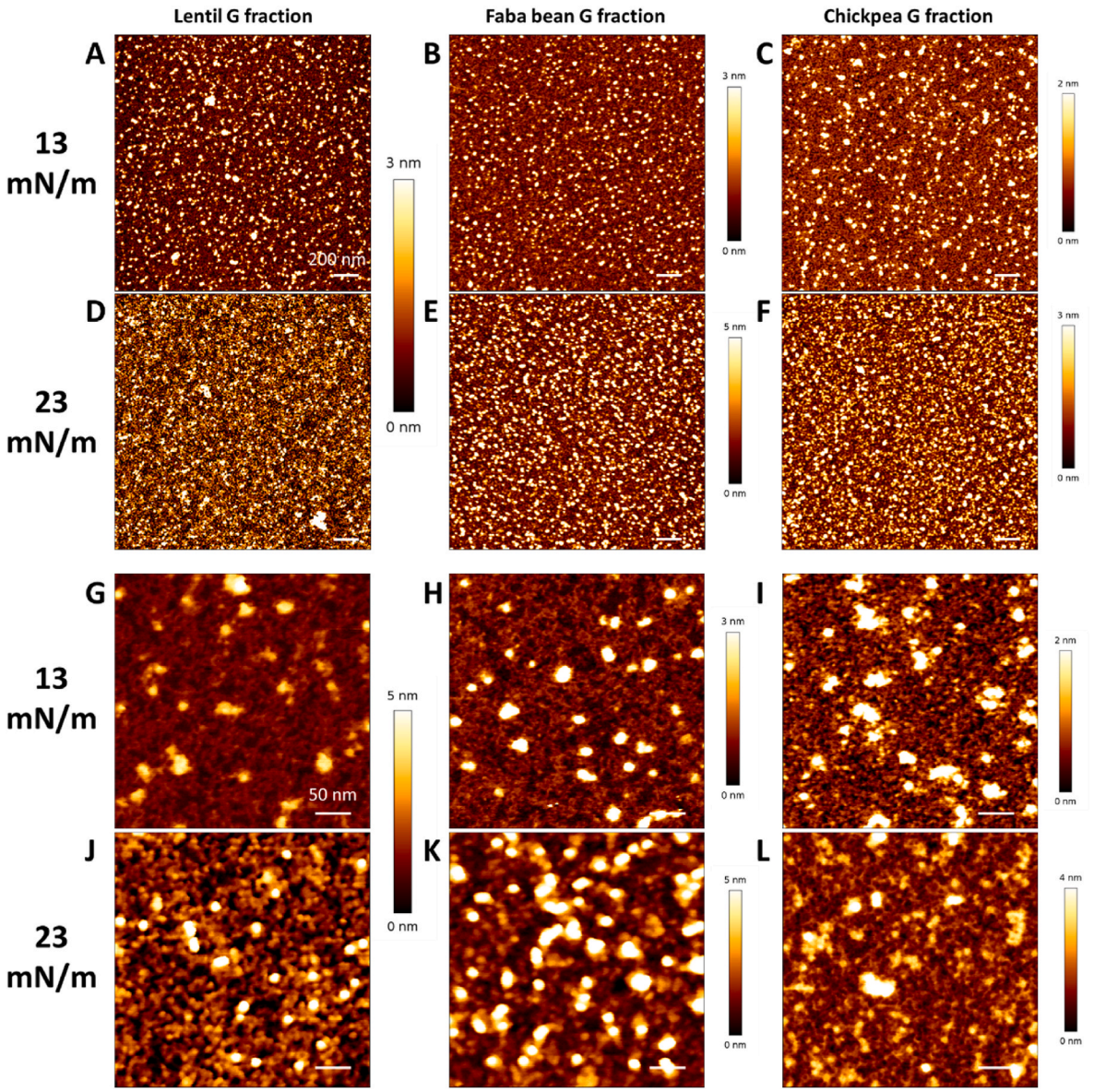

Fig. 6. AFM images of Langmuir-Blodgett films at surface pressures of 13 mN/m (A–C) and 23 mN/m (D–F) for the globulin fractions of lentil (A, D), faba bean (B, E) and chickpea (C, F) over 2 × 2 μm^2 areas in a lateral resolution of 512 × 512 pixels^2. The scale bars indicate a length of 200 nm; AFM images of Langmuir-Blodgett films at surface pressures of 13 mN/m (G–I) and 23 mN/m (J–L) for the globulin fractions of lentil (G, J), faba bean protein (H, K) and chickpea protein (I, L) over 350 × 350 nm^2 areas in a lateral resolution of 512 × 512 pixels^2. The scale bars indicate a length of 50 nm.

showed pronouncedly lower interfacial network stiffness than lentil whole protein extract (Shen et al., 2024b). This might be due to the presence of oleosomes in chickpea whole protein extract that disrupt its interfacial network structure (Yang et al., 2021).

With increasing deformation amplitude, the values for $E_{\tau 1}$ of all samples pronouncedly decrease (Fig. 5A–F), indicating the disruption of interfacial network structures. This is supported by the fact that both $U_{\tau 2}$ (Fig. 5D–I) and $U_{\tau 3}$ (Fig. 5E–J) are increasing, where the increase in $U_{\tau 2}$ points to an increase in viscous dissipation resulting from partial yielding of the network structure, and the increase in $U_{\tau 3}$ is in part linked to material exchange between interface and bulk. In expansion, large deformations create a significant amount of new area, which can lead to additional adsorption of proteins. When the timescale of deformation is shorter than the time needed for this additional protein to merge with the residual network structures, it will be expelled again from the interface upon compression. Notably, $E_{\tau 1}$ decreases to around 20 mN/m for all samples at 50% deformation amplitude, while $U_{\tau 2}$ of albumin-stabilized interfaces increase to a much larger extent than those of globulin-stabilized interfaces, indicating more severe network structure disruption for albumin-stabilized interfaces. The values for $E_{\tau 4}$ become increasingly negative when the deformation amplitude increases from 2 to 20%, suggesting an increasing interfacial resistance to density change. For all albumins, they start to become less negative again, when the deformation amplitude increases from 20% to 50%, which is reflected by the dimple formation in the τ_4 curves around zero intra-cycle strain for these proteins at a 50% deformation amplitude (Figs. S3D–F). This increase can be caused by in-plane rearrangements or additional adsorption/desorption and coincides with the strong increase in $U_{\tau 3}$ beyond 20% deformation. The globulin fractions do not show a minimum in $E_{\tau 4}$ and have significantly lower values for $U_{\tau 3}$, which could be linked to the slower rate of adsorption of the globulins (Fig. 2). The vertical shift, γ_s of all samples becomes increasingly negative with increasing strain amplitude (Fig. 5C–H), which is more pronounced for albumin-stabilized interfaces (Fig. 5H), suggesting that these interfaces are driven further out of equilibrium by the applied oscillations compared to globulin-stabilized interfaces.

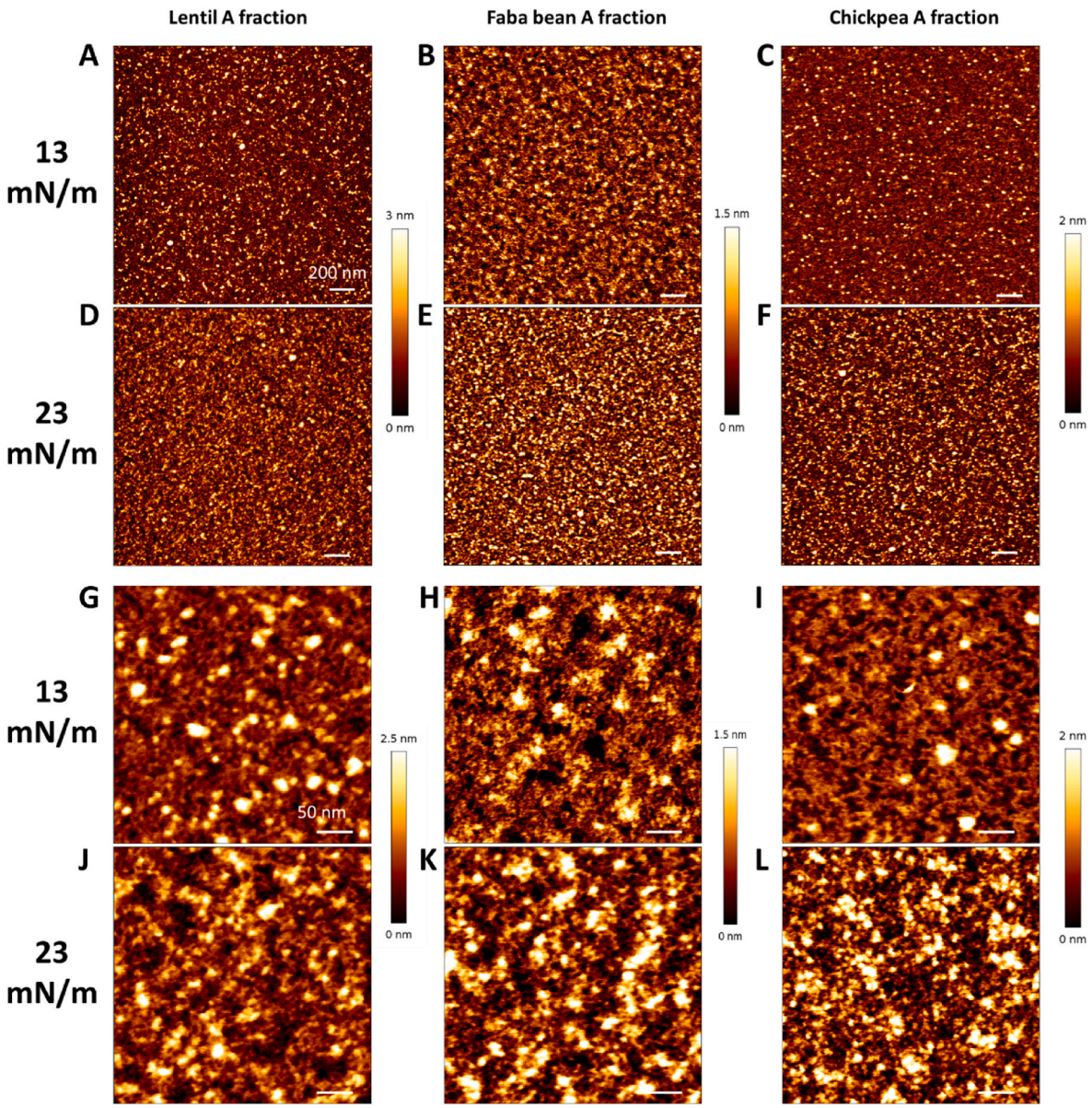

Fig. 7. AFM images of Langmuir-Blodgett films at surface pressures of 13 mN/m (A–C) and 23 mN/m (D–F) for the albumin fractions of lentil (A, D), faba bean (B, E) and chickpea (C, F) over 2 × 2 μm^2 areas in a lateral resolution of 512 × 512 $pixels^2$. The scale bars indicate a length of 200 nm; AFM images of Langmuir-Blodgett films at surface pressures of 13 mN/m (G–I) and 23 mN/m (J–L) for the albumin fractions of lentil (G, J), faba bean protein (H, K) and chickpea protein (I, L) over 350 × 350 nm^2 areas in a lateral resolution of 512 × 512 $pixels^2$. The scale bars indicate a length of 50 nm.

Comparing the individual globulin fractions, the lentil globulin-stabilized interface shares similar $E_{\tau 1}$ (Fig. 5A) and $U_{\tau 2}$ (Fig. 5D) profiles with the chickpea globulin fraction, which implies that the network structure at these two interfaces have similar response of their network to large dilatational deformations. The faba bean globulin-stabilized interface has significantly lower values for $E_{\tau 1}$. In fact, its modulus is nearly constant up to 10% deformation, indicating that the microstructure of its interface is less stiff but also less brittle. Analysis of the even harmonics shows that the lentil globulin-stabilized interface has the lowest (i.e., most negative) values for $E\tau_4$ (Fig. 5B), highest $U_{\tau 3}$ (Fig. 5E) and most negative γ_s (Fig. 5C), followed by chickpea and faba bean globulin-stabilized interfaces.

Within the albumin fractions, the lentil albumin-stabilized interface has lower values for $U_{\tau 2}$ (Fig. 5I) and a less negative value for γ_s (Fig. 5H) than the others, suggesting a lower extent of interfacial network disruption and a smaller shift from equilibrium for the lentil albumin fraction. The chickpea albumin-stabilized interface shows a higher $U_{\tau 3}$ at 50% deformation amplitude than the others (Fig. 5J), which indicates a higher extent of interface-bulk exchange, ascribed to the faster interfacial adsorption of the chickpea albumin fraction (Fig. 2D).

In short, all pulse globulin and albumin fractions formed disordered solid-like interfaces, and their interfacial network structures are mainly responsible for their interfacial rheological behavior in dilatational deformation. Albumin-stabilized interfaces are much stiffer while more brittle than globulin-stabilized interfaces. In the next section we will discuss how these differences are linked to the microstructure of the interface.

3.5. *Langmuir-Blodgett film imaging and image analysis*

The interfacial structures of globulin and albumin fractions were characterized by imaging Langmuir-Blodgett films prepared at 13 and 23 mN/m surface pressures with AFM, using the same method we employed for whole pulse protein extracts (Shen et al., 2024b). The high

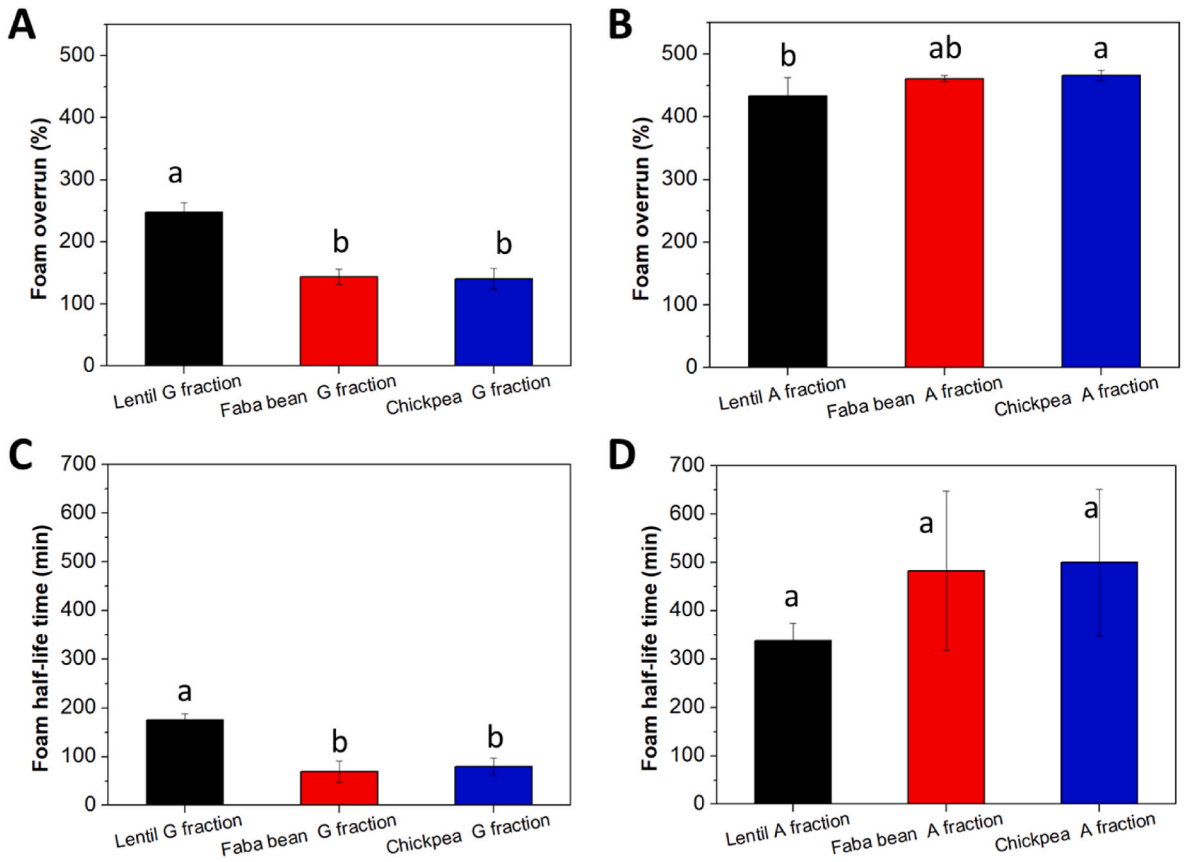

Fig. 8. Foam overrun (A, C) and foam half-life time (B, D) of the globulin and albumin fractions from lentil, faba bean and chickpea, respectively. Protein dispersions containing 0.1% (w/w) soluble protein were prepared in phosphate buffer (20 mM, pH7) at 20 °C and filtrated through 0.22 μm filters. The averages and standard deviations were the results of at least three replicates. Columns with different letters are significantly different ($p < 0.05$).

surface pressure is close to the surface pressure reached after 3 h of adsorption, and the lower value is representative of an expanded state. In the AFM images, bright parts indicate protein-rich domains (Figs. 6 and 7). In the 2 × 2 μm^2 images (Fig. 6A–F; Fig. 7A–F), all films are disordered and heterogeneous at both 13 and 23 mN/m surface pressures, agreeing with the weak dependency of the dilatational moduli of these interfaces on frequency in the dilatational rheology (Fig. 3A–C).

The films were subjected to image analysis to determine the protein domain size using pair correlation function analysis, and to characterize the protein network features by using the software Angiotool 64, according to our previous study (Shen et al., 2024a). From analysis of the pair correlation function, the maxima of g(r) of albumin films are mostly smaller than those of globulin films (Table S3), but here is no significant ($p < 0.05$) difference among the maxima of g(r) between albumin films (Table S3), implying comparable structural heterogeneity of these films independent of surface pressures and albumin species. As for globulin films, higher surface pressure leads to the decrease in the heterogeneity of lentil globulin films, as indicated by its significant ($p < 0.05$) decrease in the maximum of g(r) (Table S3). Globulin films tend to have larger protein domain size than albumin films (Table S3), while there are hardly significant ($p < 0.05$) differences between them. Overall, these films have protein domain sizes between 55 and 75 nm, which probably indicate the size of the primary aggregates formed by these proteins that constitute the overall interfacial network structures. These protein domain sizes are comparable to those of the whole protein extracts (60–78 nm) (Shen et al., 2024b). Interestingly, those sizes are also comparable to the characteristic size of the protein aggregates (~60 nm) formed in heat-set pea protein gels (Munialo, van der Linden, Ako, & de Jongh, 2015), which points out possible similarities between interfacial network structure and bulk network structure of pulse proteins.

According to the network analysis, at a surface pressure of 13 mN/m, all albumin films have higher surface coverage (51.8–56.9%) than corresponding globulin films (48.4–51.6%) (Table S4), and they also tend to have higher junction density, longer average vessel length, lower Lacunarity, higher branching rate and lower end-point rate, suggesting the higher capability of pulse albumin proteins in creating dense and fine interfacial network structures than pulse globulins. At a surface pressure of 23 mN/m, lentil and chickpea globulin films have comparable structural parameters to those of the corresponding albumin films (Table S4), whereas the increase of surface pressure barely influences the network structural parameters of faba bean globulin and chickpea albumin films (Table S4). Within globulin films, lentil and chickpea globulin films both have higher vessel area and junction density, longer average vessel length, lower lacunarity, higher branching rate and lower end-point rate than faba bean globulin films at surface pressure of 23 mN/m (Table S4), suggesting higher surface coverage and surface connectivity, longer protein threads, a finer structure, and higher level of structural branching of these films. The higher level of development of the interfacial network structure and higher surface coverage for lentil and chickpea globulins contribute to a higher resistance of these interfaces in dilatational deformation to both interfacial network (Fig. 5A) and density changes (Fig. 5B), compared to faba bean globulin. The albumin films show superior network structural properties at 23 mN/m surface pressure than globulin films (Table S4), contributing to the overall higher resistance of the interfaces stabilized by the albumin proteins to both small and large dilatational deformations (Fig. 7).

3.6. Foaming properties

The foaming properties including foamability and foam stability

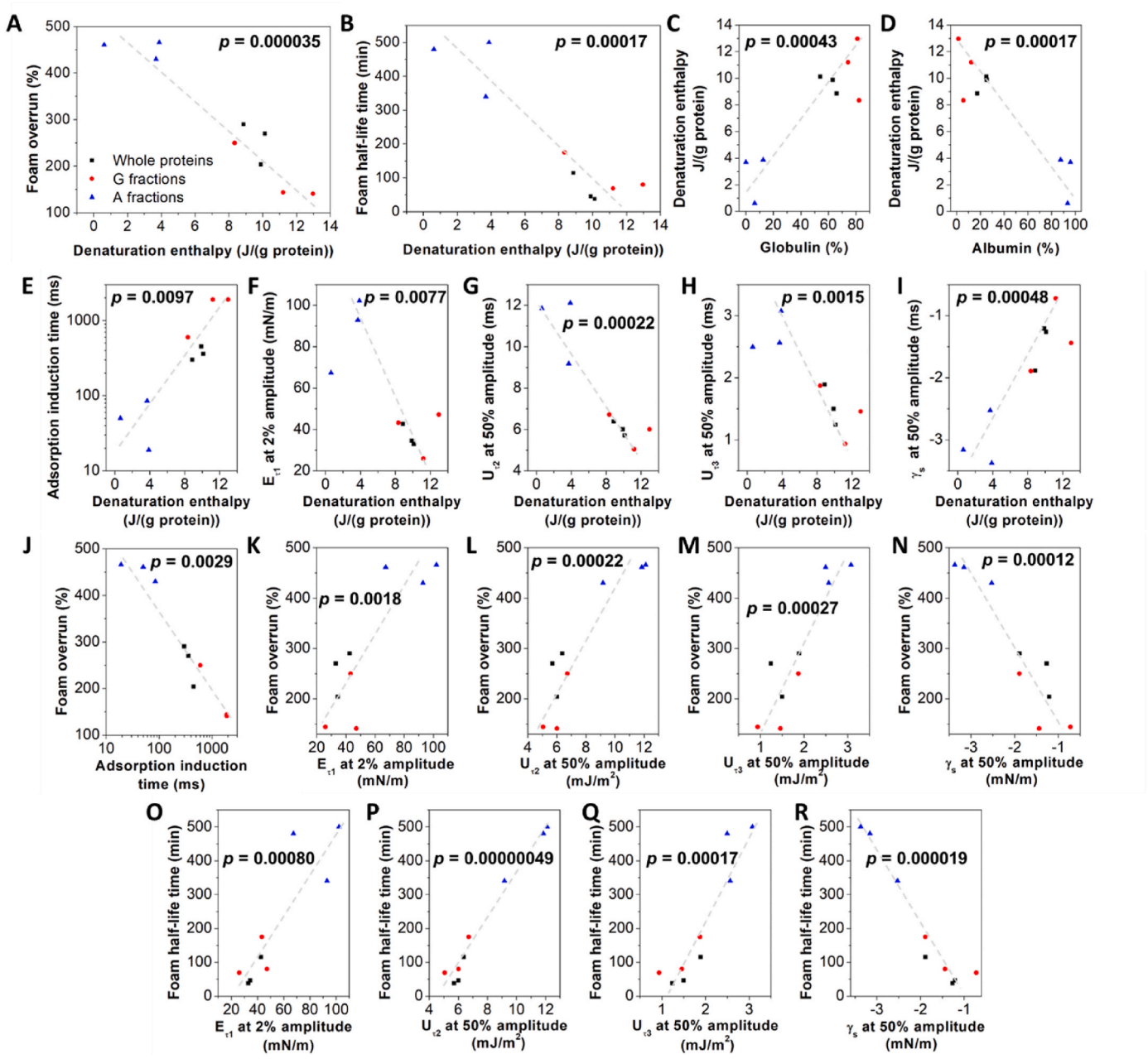

Fig. 9. Relationship between key molecular and interfacial properties of pulse proteins and their foamability and foam stability properties. Grey lines are guides for the eye.

were evaluated for the globulin and albumin fractions by measuring their foam overrun and foam half-life time.

3.6.1. Foamability

Albumin fractions have foam overruns between 433% and 466% (Fig. 8B), which are much higher than those of globulin fractions (141–248%) (Fig. 8A). The foam overruns of albumins and globulins follow this order: chickpea albumin > faba albumin > lentil albumin ≫ lentil globulin > faba bean globulin ≈ chickpea globulin. This order highly aligns with that of their induction time for adsorption at the air-water interface (Fig. 2A–D), indicating the crucial role of adsorption induction time in the foamability of pulse proteins. Additionally, for albumin fractions the interfacial stiffness develops faster than for globulin fractions (Fig. 2C–F), which is also in favor of foamability by stabilizing the newly generated air bubbles during foaming. According to our previous study (Shen et al., 2024b), the foam overruns of lentil, faba bean and chickpea whole protein extracts lie in the middle of those of corresponding albumin and globulin fractions, indicating the positive contributions of albumin fractions in the foamability of those whole protein extracts. Especially, the foam overrun of chickpea globulin fraction (141%) is much lower than chickpea whole protein extract (270%) (Fig. 8A), although the latter only contains 26% albumin proteins, suggesting that the presence of albumins can significantly enhance the foamability of chickpea proteins.

3.6.2. Foam stability

Regarding foam stability, all albumin fractions also have much longer foam half-life time (339–500 min) than all globulin fractions (69–175 min) (Fig. 8C and D), which is attributed to the stiffer (Fig. 3; Fig. 5A–F) and finer (Tables S3 and S3) network structures they form at the interface. There are no differences in the foam half-life time of albumin fractions (p = 0.097), in line with their similar interfacial

Table 2
Correlation matrix (correlation coefficient and *p* value) between protein molecular properties, indicative parameters of interfacial rheological properties and structural properties, and foaming properties of the whole, globulin and albumin fractions of lentil, faba bean and chickpea.

	Globulin content	Vicilin and convicilin content	Albumin content	Peak particle size	Zeta potential	H_0	Denaturation enthalpy
Globulin content	1						
Vicilin and convicilin content	.858[b]	1					
Albumin content	−.994[b]	−.841[b]	1				
Peak particle size	.726[a]	.682[a]	−.665[a]	1			
Zeta potential	−.950[b]	−.931[b]	.946[b]	−.745[a]	1		
H0	.589[a]	.856[b]	−0.581	0.333	−.649[a]	1	
Denaturation enthalpy	.903[b]	.612[a]	−.926[b]	0.521	−.785[b]	0.383	1
Adsorption induction time	.685[a]	0.318	−.673[a]	0.515	−0.512	−0.004	.752[b]
$E_{\tau 1}$ at 2% amplitude	−.844[b]	−.652[a]	.862[b]	−0.411	.803**	−0.361	−.769[b]
$E_{\tau 1}$ at 50% amplitude	−0.385	0.031	0.422	0.031	0.226	0.311	−0.534
$E_{\tau 4}$ at 50% amplitude	−0.428	−.729*	0.419	−0.579	.621[a]	−.644[a]	−0.223
$U_{\tau 2}$ at 50% amplitude	−.865[b]	−.628[a]	.899[b]	−0.469	.811[b]	−0.326	−.920[b]
$U_{\tau 3}$ at 50% amplitude	−.806[b]	−0.499	.837[b]	−0.320	.697[a]	−0.208	−.860[b]
γ_s at 50% amplitude	.812[b]	0.499	−.841[b]	0.386	−.705[a]	0.201	.899[b]
Maximum of g(r)	0.495	0.093	−0.461	0.384	−0.281	−0.166	0.553
Vessel area	−0.012	0.330	0.002	0.078	−0.230	0.324	−0.266
Junction density	−0.226	0.164	0.240	−0.057	0.062	0.294	−0.517
Vessel length	−0.209	0.063	0.179	−0.274	0.023	0.134	−0.401
Lacunarity	0.251	−0.111	−0.245	0.169	−0.080	−0.249	0.492
Branching Rate	−0.325	0.042	0.350	−0.134	0.228	0.244	−.590[a]
EndPoint Rate	0.110	−0.250	−0.090	0.048	0.114	−0.327	0.328
Foam overrun	−.925[b]	−.610[a]	.930[b]	−.617[a]	.798[b]	−0.287	−.953[b]
Foam half-life time	−.852[b]	−.596[a]	.892[b]	−0.420	.787[b]	−0.329	−.926[b]

[a] $p < 0.05$.
[b] $p < 0.01$.

structures (Fig. 7; Tables S3 and S3). As for the globulins, lentil has the longest foam half-life time (175 min) compared to faba bean (69 min) and chickpea (80 min) (Fig. 8C). Lentil globulin-stabilized interfaces displayed higher interfacial network stiffness than faba bean globulin-stabilized interfaces (Fig. 5A) and higher resistance to interfacial density changes (Fig. 5B) than both faba bean and chickpea globulin-stabilized interfaces. Hence, lentil globulin fraction-stabilized foam is more resistive to bubble rupture that highly involves dilatational deformations (A. Bos & van Vliet, 2001; J. Wang, Nguyen, & Farrokhpay, 2016). Besides, the lentil globulin fraction has higher surface charge than both faba bean and chickpea globulins (Table 1), which can cause higher electrostatic repulsion forces between air bubbles that could also reduce their coalescence. Compared to lentil globulin, faba bean globulin has an interfacial structure which is less dense, less connective, has shorter protein threads, is less fine and has less branching (Tables S3 and S3). These properties likely result in the low interfacial resistance of faba bean globulin to dilatational deformation (Fig. 3; Fig. 5A and B), and therefore all these attributes result in the much lower foam stability of faba bean globulin compared to lentil globulin.

Counterintuitively, chickpea globulin has comparably low foam stability to faba bean globulin (Fig. 8C) even though the chickpea globulin-stabilized interface is much stiffer than the faba bean globulin-stabilized interface at small deformation amplitudes (e.g. 2% strain) (Fig. 3; Fig. 5A). As shown in Figs. 5A and 6B, these two interfaces display similar residual network stiffness and resistance to interfacial density change at large deformation amplitudes (e.g. 50%), which suggests the significant role of the interfacial rheological behavior of pulse globulin proteins at large deformations in their foam stabilization properties. Both lentil (175 min) and chickpea (80 min) globulin fractions have pronouncedly higher foam half-life time than the corresponding lentil (115 min) and chickpea (38 min) whole protein extracts according to our previous study (Shen et al., 2024b). As for the lentil globulin fraction, it formed an interface with slightly higher interfacial stiffness (E_d' = 45.4 mN/m versus 43.8 mN/m at 2% deformation amplitude) and smaller protein clusters (64 nm versus 76 nm) compared to its whole protein extract. It also displayed more intermolecular connections (junction density of 367 junctions/μm^2 versus 339 junctions/μm^2) and higher level of branching (branching rate of 631 versus 559). These properties are expected to result in a higher foam stability of lentil globulin fraction. Regarding chickpea globulins, they have pronouncedly higher interfacial stiffness (E_d' = 46.5 mN/m) than chickpea whole protein extract (E_d' = 32.5 mN/m) at 2% deformation amplitude, which can explain its higher foam stability compared to chickpea whole protein extract during aging of the foam.

3.7. Relationship between the molecular, interfacial and foaming properties of pulse proteins

In this section, we comprehensively analyzed the links between the molecular, interfacial and foaming properties of lentil, faba bean and chickpea globulin and albumin fractions measured above, including the data of the whole protein extracts from our previous study, using correlation analysis. These analyses aim to search for the key parameters that highly influence the foaming properties of pulse proteins.

Overall, the denaturation enthalpy seems to be one of the key molecular properties of pulse proteins. Pulse proteins with higher content of globulins tend to have a higher value of the denaturation enthalpy ($p = 4.3 \times 10^{-4}$), and the contrary is true for the content of albumins ($p = 1.7 \times 10^{-4}$) (Fig. 9C and D; Table 2). Lower denaturation enthalpy is highly correlated to higher foam overrun ($p = 3.5 \times 10^{-5}$), and higher foam half-life time ($p = 1.7 \times 10^{-4}$) of the pulse proteins (Fig. 9A and B; Table 2). Lower denaturation enthalpy implies lower conformational stability of protein molecules, which may indicate that the protein molecules can rearrange their structures more easily. Presumably this can result in a higher extent or rate of structural rearrangement at the interface, therefore resulting in higher efficiency in increasing interfacial pressure and a lower adsorption induction time ($p = 9.7 \times 10^{-3}$) (Fig. 9E), and consequently a higher foamability ($p = 2.9 \times 10^{-3}$) (Fig. 9J) (Table 2). Such effects of low denaturation enthalpy could also increase the protein-protein in-plane interactions ($p = 7.7 \times 10^{-3}$) (Fig. 9F), and hence the formation of interfacial network structure ($p = 2.2 \times 10^{-4}$) (Fig. 9G) and the response to interfacial density changes ($p < 2 \times 10^{-3}$) (Fig. 9H and I) (Table 2). These factors are conducive to the stability of air bubbles during preparation and aging, and tend to cause

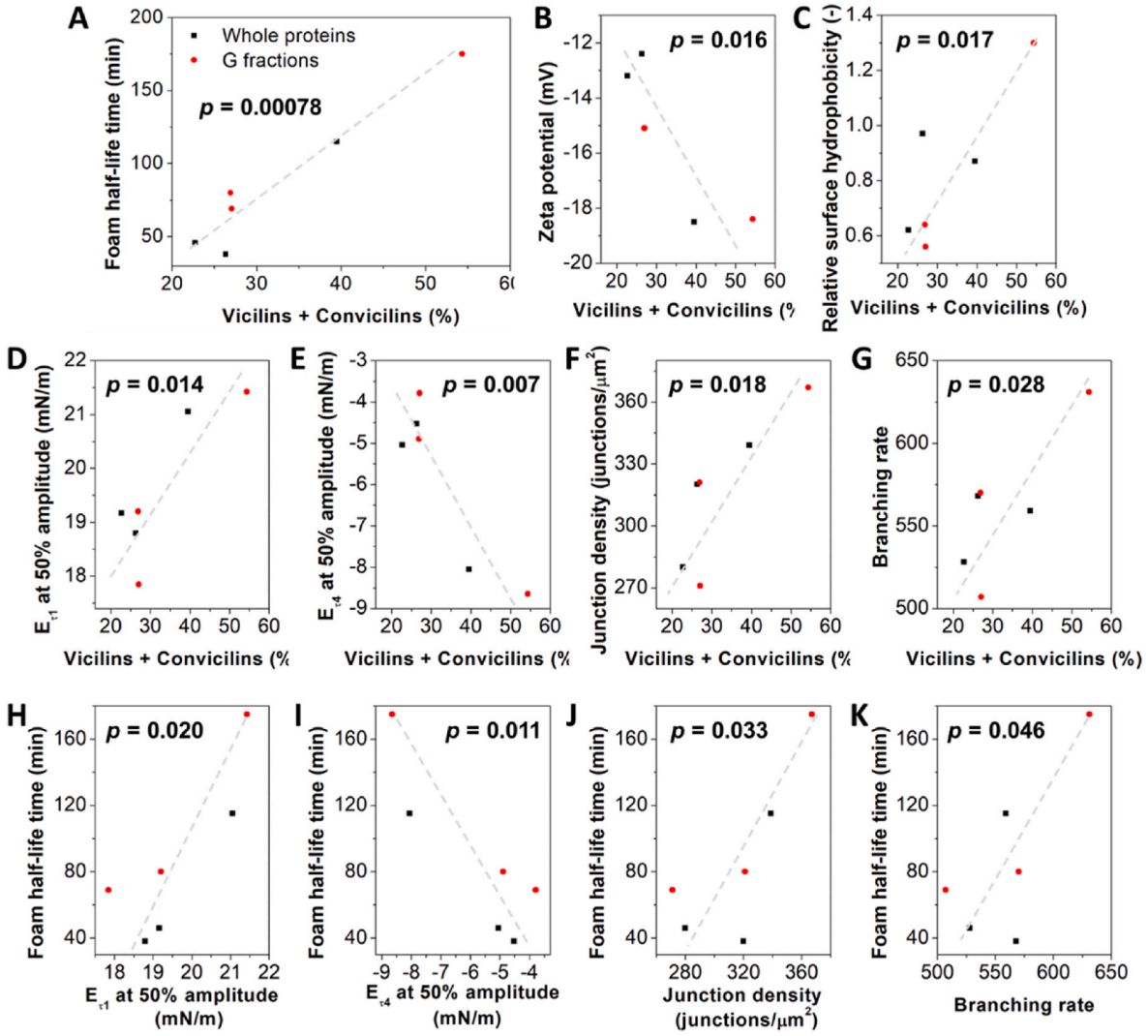

Fig. 10. Relationship between the molecular and interfacial properties of vicilins and convicilins from whole and globulin fractions and their foam stability. Grey lines are guides for the eye.

both high foamability ($p < 2 \times 10^{-3}$) (Fig. 9K–N) and high foam stability of pulse proteins ($p < 8 \times 10^{-4}$) (Fig. 9O–R) (Table S6).

For globulin-rich pulse proteins, a high content of vicilins and convicilins is highly correlated to long foam half-life time ($p = 7.8 \times 10^{-4}$) (Fig. 10A), partially given by the introduction of a higher value of the zeta potential ($p = 1.6 \times 10^{-2}$) (Fig. 10B), that could cause stronger electrostatic repulsion between air bubbles (Table S5). Higher contents of vicilins and convicilins are also prone to introduce higher surface hydrophobicity ($p = 1.7 \times 10^{-2}$) (Fig. 10C; Table S5). It might increase the interfacial load of pulse proteins by promoting their adsorption to the interface and leads to higher interfacial resistance to interfacial density changes (Fig. 10E). High surface hydrophobicity might also promote the formation of interfacial network structures (Fig. 10F and G) that cause higher residual interfacial stiffness at large deformation (Fig. 10D). Finally, these factors tend to enhance the foam stability of globulin-rich pulse proteins ($p < 5 \times 10^{-2}$) (Fig. 10H–K) and are the features of the lentil globulin fraction.

As for legumins, high content of legumins is highly correlated to low foamability ($p = 6.7 \times 10^{-3}$) (Fig. 11A). This is because on the one hand, it tends to introduce lower surface hydrophobicity ($p = 4.6 \times 10^{-2}$) (Fig. 11B) that decreases the affinity of pulse proteins to the air-water interface and prolongs the adsorption induction time ($p = 3.5 \times 10^{-2}$) (Fig. 11C) (Table S5). On the other hand, higher content of legumins are prone to disrupting the interfacial structures by increasing the heterogeneity ($p = 7.2 \times 10^{-3}$) (Fig. 11D) and decrease the length of protein threads in the interfacial network structure ($p = 1.5 \times 10^{-2}$) (Fig. 11E), which might be detrimental to the stability of air bubbles during early formation and consequently decrease the foamability ($p < 2.2 \times 10^{-2}$) (Fig. F,G). Hence, for globulin-rich pulse proteins, vicilins (plus convicilins) seem to dominate their foam stability, while legumins seem to dominate their foamability.

In interfacial measurements proteins adsorb to the interface primarily driven by diffusion, which is different from the foaming measurements, where there may also be a convective contribution to transport to the interface. But despite the flow induced by whipping, boundary layers may form close to the air-water interface across which there is still a significant contribution from diffusion. This may be the reason why the interfacial tensiometry data still correlate well with the foaming data.

4. Conclusion

In this study, we systematically studied the individual roles of globulins and albumins from lentils, faba beans and chickpeas in air-water interface and foam stabilization. All albumin fractions overall displayed much higher foamabilities with foam overrun of 430–466%

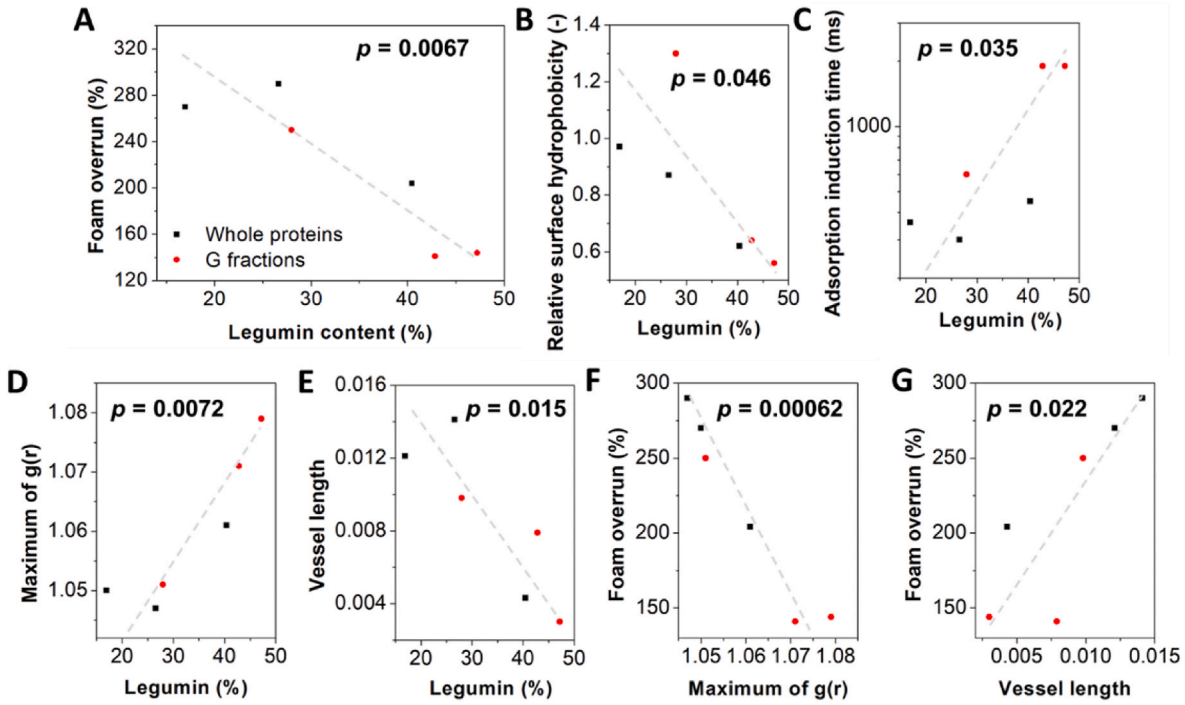

Fig. 11. Relationship between the molecular and interfacial properties of legumins from whole and globulin fractions and their foamability. Grey lines are guides for the eye.

than all globulin fractions (141–250%), and they could pronouncedly increase the foamabilities of the whole pulse protein extracts (204–290%) although they were only the minor fractions. The albumin fractions also had much higher foam stabilities with foam half-life time of 340–500 min compared to the globulin fractions (80–175 min), but globulin fractions dominated the foam stabilities of the whole pulse protein extracts (38–115 min), since they were the major components present in the mixture. By performing correlation analysis, we found that denaturation enthalpy is a key parameter highly influencing the foaming properties of pulse proteins. Lower denaturation enthalpy of pulse proteins appears to be linked to higher foamability and higher foam stability, due to the greater conformational flexibility that allows for a faster adsorption rate at the air-water interface, and may result in a higher degree of structural rearrangement at the interface, which is a feature of pulse albumins. This can increase the stiffness of the interfacial network structure.

For globulin-rich pulse proteins, vicilins and convicilins seem conducive to foam stability by forming stiff interface and developing interfacial network structure, which increase the interfacial resistance to large deformation and enhance foam stability. High content of vicilins and convicilins also tend to bring high surface charge and promote foam stability by increasing electrostatic repulsion forces between air bubbles. Legumins tend to reduce foamability since they tend to have low surface hydrophobicity and adsorb on the air-water interface slowly, and they seem to disrupt the interfacial structure by increasing interfacial heterogeneity and decreasing the length of protein threads in the interfacial network structure.

The above correlation analysis was based on original whole protein extracts and isolated globulin fractions and albumin fractions from only three pulses: lentil, faba bean and chickpea, and the whole protein extracts overall displayed behavior much more similar to the isolated globulin fractions due to their abundance in the mixtures. Therefore, the behavior of more pulse proteins with moderately higher albumin contents are suggested for further investigation, for example, by mixing globulins and albumins at different ratios, to solidify the above correlation analysis. This study unraveled several important parameters in terms of molecular properties and interfacial properties of pulse proteins for the preparation and stabilization of foam. These findings might also be helpful in modelling and theory establishment to further describe and predict the interfacial and foaming behavior of pulse proteins.

CRediT authorship contribution statement

Penghui Shen: Writing – original draft, Visualization, Validation, Methodology, Investigation, Conceptualization. **Solange M.L. Ha:** Writing – review & editing, Investigation. **Jinfeng Peng:** Writing – review & editing. **Jasper Landman:** Writing – review & editing, Supervision, Methodology, Conceptualization. **Leonard M.C. Sagis:** Writing – review & editing, Supervision, Methodology, Conceptualization.

Declaration of competing interest

The authors have declared that no competing interest exists. This manuscript has not been published and is not under consideration for publication in any other journal. All authors approve this manuscript and its submission to Food Hydrocolloids.

Acknowledgements

Authors acknowledge Danone Research & Innovation for the financial support and Joerg Barner for capturing the AFM images of LPI films. P. Shen acknowledges the funding from China Scholarship Council (CSC NO. 202006150032).

Appendix A. Supplementary data

Supplementary data to this article can be found online at https://doi.org/10.1016/j.foodhyd.2024.110792.

Data availability

Data will be made available on request.

References

Bos, M. A., & van Vliet, T. (2001). Interfacial rheological properties of adsorbed protein layers and surfactants: A review. *Advances in Colloid and Interface Science, 91*(3), 437–471.

Adarsh, S., Jacob, J., & Giffy, T. (2019). Role of pulses in cropping systems: A review. *Agricultural Reviews, 40*(3), 185–191.

Alabi, O. O., Ali, N., Nwachukwu, I. D., Aluko, R. E., & Amonsou, E. O. (2020). Composition and some functional properties of Bambara groundnuts vicilin fraction. *Lebensmittel-Wissenschaft und -Technologie, 125*, Article 109256.

Alfieri, F., Ververis, E., Precup, G., Julio-Gonzalez, L. C., & Noriega Fernández, E. (2023). Proteins from pulses: Food processing and applications. In P. Ferranti (Ed.), *Sustainable food science - a comprehensive approach* (pp. 192–218). Oxford: Elsevier.

Baziwane, D., & He, Q. (2003). Gelatin: The paramount food additive. *Food Reviews International, 19*(4), 423–435.

Boukid, F., Zannini, E., Carini, E., & Vittadini, E. (2019). Pulses for bread fortification: A necessity or a choice? *Trends in Food Science & Technology, 88*, 416–428.

Chandran, A. S., Suri, S., & Choudhary, P. (2023). Sustainable plant protein: An up-to-date overview of sources, extraction techniques and utilization. *Sustainable Food Technology, 1*(4), 466–483.

Chen, Y., McGee, R., Vandemark, G., Brick, M., & Thompson, H. J. (2016). Dietary fiber analysis of four pulses using AOAC 2011.25. *Implications for Human Health, 8*(12), 829.

Cserhalmi, Z., Czukor, B., & Gajzágó-Schuster, I. (1998). Emulsifying properties, surface hydrophobicity and thermal denaturation of pea protein fractions. *Acta Alimentaria, 27*(4), 357–363.

Dagorn-Scaviner, C., Gueguen, J., & Lefebvre, J. (1986). A comparison of interfacial behaviours of pea (Pisum sativum L.) legumin and vicilin at air/water interface. *Food, 30*(3–4), 337–347.

de Groot, A., Yang, J., & Sagis, L. M. C. (2023). Surface stress decomposition in large amplitude oscillatory interfacial dilatation of complex interfaces. *Journal of Colloid and Interface Science, 638*, 569–581.

Dhull, S. B., Kidwai, M. K., Noor, R., Chawla, P., & Rose, P. K. (2022). A review of nutritional profile and processing of faba bean (Vicia faba L.). *Legume Science, 4*(3), Article e129.

Emre, İ., Turgut-balık, D., Genç, H., & Şahin, A. (2015). Determination of genetic variations in lathyrus L. Species based on SDS-PAGE analyses of seed storage proteins (albumin, globulin A, glutelin). *Turkish Journal of Science and Technology, 10*(1), 21–26.

Flachowsky, G., Meyer, U., & Südekum, K. H. (2018). Invited review: Resource inputs and land, water and carbon footprints from the production of edible protein of animal origin. *Archives of Animal Breeding, 61*(1), 17–36.

González-Pérez, S., & Arellano, J. B. (2009). Vegetable protein isolates. In G. O. Phillips, & P. A. Williams (Eds.), *Handbook of Hydrocolloids* (2nd ed., pp. 383–419). Woodhead Publishing.

Gravel, A., & Doyen, A. (2023). Pulse globulins 11S and 7S: Origins, purification methods, and Techno-functional properties. *Journal of Agricultural and Food Chemistry, 71*(6), 2704–2717.

Hall, A. E., & Moraru, C. I. (2021). Structure and function of pea, lentil and faba bean proteins treated by high pressure processing and heat treatment. *Lebensmittel-Wissenschaft und -Technologie, 152*, Article 112349.

Jarpa-Parra, M., Wong, L., Wismer, W., Temelli, F., Han, J., Huang, W., et al. (2017). Quality characteristics of angel food cake and muffin using lentil protein as egg/milk replacer. *International Journal of Food Science and Technology, 52*(7), 1604–1613.

Khiangte, Z., & Siddique, A. (2021). Pulse crops: Steps towards the sustainability in agriculture. *International Journal of Communication Systems, 9*(1), 487–490.

Kokkinidis, M., Glykos, N. M., & Fadouloglou, V. E. (2012). Chapter 7 - protein flexibility and Enzymatic catalysis. In C. Christov, & T. Karabencheva-Christova (Eds.), *Advances in protein Chemistry and structural biology* (Vol. 87, pp. 181–218). Academic Press.

Krishnan, H. B., & Coe, E. H. (2001). Seed storage proteins. In S. Brenner, & J. H. Miller (Eds.), *Encyclopedia of genetics* (pp. 1782–1787). New York: Academic Press.

Kuang, J. (2022). Study of the interactions and physicochemical properties of pea and egg white protein mixtures : from the colloidal to the gelled state; Etude des interactions et des propriétés physico-chimiques de mélanges de protéines de pois et de blanc d'oeuf : de l'état colloidal à l'état gélifié. *Université Bourgogne Franche-Comté*.

Kumar, S., & Pandey, G. (2020). Biofortification of pulses and legumes to enhance nutrition. *Heliyon, 6*, Article e03682.

Lucassen, J., & Van Den Tempel, M. (1972). Dynamic measurements of dilational properties of a liquid interface. *Chemical Engineering Science, 27*(6), 1283–1291.

Ma, K. K., Greis, M., Lu, J., Nolden, A. A., McClements, D. J., & Kinchla, A. J. (2022). Functional performance of plant proteins. *Foods, 11*.

Ma, X., Shen, P., Habibi, M., & Sagis, L. M. C. (2024). Interfacial properties and functionality of lupin protein-pectin complexes at the air-water interface. *Food Hydrocolloids, 154*, Article 110050.

McClements, D. J., & Grossmann, L. (2021). A brief review of the science behind the design of healthy and sustainable plant-based foods. *Npj Science of Food, 5*(1), 17.

Mistry, K., Sardar, S. D., Alim, H., Patel, N., Thakur, M., Jabbarova, D., et al. (2022). Plant based proteins: Sustainable alternatives. *Plant Science Today, 9*(4), 820–828.

Mitropoulos, V., Mütze, A., & Fischer, P. (2014). Mechanical properties of protein adsorption layers at the air/water and oil/water interface: A comparison in light of the thermodynamical stability of proteins. *Advances in Colloid and Interface Science, 206*, 195–206.

Munialo, C. D., van der Linden, E., Ako, K., & de Jongh, H. H. J. (2015). Quantitative analysis of the network structure that underlines the transitioning in mechanical responses of pea protein gels. *Food Hydrocolloids, 49*, 104–117.

Murray, B. S. (2020). Recent developments in food foams. *Current Opinion in Colloid & Interface Science, 50*, Article 101394.

Nasrollahzadeh, M., Nezafat, Z., & Shafiei, N. (2021). Chapter 3 - proteins in food industry. In M. Nasrollahzadeh (Ed.), *Biopolymer-based metal nanoparticle chemistry for sustainable applications* (pp. 97–136). Elsevier.

Negi, A. S., & Osuji, C. O. (2010). Time-resolved viscoelastic properties during structural arrest and aging of a colloidal glass. *Physical Review E, 82*(3), Article 031404.

Newcomer, M. E., & Brash, A. R. (2015). The structural basis for specificity in lipoxygenase catalysis. *Protein Science, 24*(3), 298–309.

Osemwota, E. C., Alashi, A. M., & Aluko, R. E. (2022). Physicochemical and functional properties of albumin, globulin and glutelin fractions of green lentil seed. *International Journal of Food Science and Technology, 57*(7), 3967–3981.

Poore, J., & Nemecek, T. (2018). Reducing food's environmental impacts through producers and consumers. *Science, 360*(6392), 987–992.

Raikos, V., Neacsu, M., Russell, W., & Duthie, G. (2014). Comparative study of the functional properties of lupin, green pea, fava bean, hemp, and buckwheat flours as affected by pH. *Food Science and Nutrition, 2*(6), 802–810.

Sagis, L. M. C., & Scholten, E. (2014). Complex interfaces in food: Structure and mechanical properties. *Trends in Food Science & Technology, 37*(1), 59–71.

Sha, L., & Xiong, Y. L. (2022). Comparative structural and emulsifying properties of ultrasound-treated pea (Pisum sativum L.) protein isolate and the legumin and vicilin fractions. *Food Research International, 156*, Article 111179.

Sharif, H. R., Williams, P. A., Sharif, M. K., Abbas, S., Majeed, H., Masamba, K. G., et al. (2018). Current progress in the utilization of native and modified legume proteins as emulsifiers and encapsulants – a review. *Food Hydrocolloids, 76*, 2–16.

Shen, Q., Li, J., Shen, X., Zhu, X., Dai, J., Tang, C., et al. (2023). Linear and nonlinear interface rheological behaviors and structural properties of pea protein (vicilin, legumin, albumin). *Food Hydrocolloids, 139*, Article 108500.

Shen, P., Peng, J., Sagis, L. M. C., & Landman, J. (2024a). Air-water interface properties and foam stabilization by mildly extracted lentil protein. *Food Hydrocolloids, 147*, Article 109342.

Shen, P., Peng, J., Sagis, L. M. C., & Landman, J. (2024b). Molecular, interfacial and foaming properties of pulse proteins. *Food Hydrocolloids, 156*, Article 110313.

Shen, P., Yang, J., Nikiforidis, C. V., Mocking-Bode, H. C. M., & Sagis, L. M. C. (2023). Cruciferin versus napin – air-water interface and foam stabilizing properties of rapeseed storage proteins. *Food Hydrocolloids, 136*, Article 108300.

Shevkani, K., Singh, N., Chen, Y., Kaur, A., & Yu, L. (2019). Pulse proteins: Secondary structure, functionality and applications. *Journal of Food Science and Technology, 56*(6), 2787–2798.

Shewry, P. R., & Casey, R. (1999). Seed proteins. In P. R. Shewry, & R. Casey (Eds.), *Seed proteins* (pp. 1–10). Netherlands: Springer. Dordrecht.

Shohat, D., Friedman, Y., & Lahini, Y. (2023). Logarithmic aging via instability cascades in disordered systems. *Nature Physics, 19*(12), 1890–1895.

Shrestha, S., van 't Hag, L., Haritos, V. S., & Dhital, S. (2023). Lentil and Mungbean protein isolates: Processing, functional properties, and potential food applications. *Food Hydrocolloids, 135*, Article 108142.

Snyder, C. S., Bruulsema, T. W., Jensen, T. L., & Fixen, P. E. (2009). Review of greenhouse gas emissions from crop production systems and fertilizer management effects. *Agriculture, Ecosystems & Environment, 133*(3), 247–266.

Švachulova, J., Turkova, V., & Klozová, E. (1982). The separation and comparison of albumin complexes of seed proteins in three cultivars ofPhaseolus vulgaris. *Biologia Plantarum, 24*(2), 81–88.

Tang, C.-H. (2017). Emulsifying properties of soy proteins: A critical review with emphasis on the role of conformational flexibility. *Critical Reviews in Food Science and Nutrition, 57*(12), 2636–2679.

Varasundharosoth, D., & Barnes, M. F. (1985). The isolation and amino acid composition of some proteins from the albumin complex of seed of Lupinus angustifolius L. Cv. Uniharvest. *Journal of Plant Physiology, 120*(2), 131–144.

Vogelsang-O'Dwyer, M., Zannini, E., & Arendt, E. K. (2021). Production of pulse protein ingredients and their application in plant-based milk alternatives. *Trends in Food Science & Technology, 110*, 364–374.

Wang, J., Nguyen, A. V., & Farrokhpay, S. (2016). A critical review of the growth, drainage and collapse of foams. *Advances in Colloid and Interface Science, 228*, 55–70.

Wang, N., & Toews, R. (2011). Certain physicochemical and functional properties of fibre fractions from pulses. *Food Research International, 44*(8), 2515–2523.

Wierenga, P. A., & Gruppen, H. (2010). New views on foams from protein solutions. *Current Opinion in Colloid & Interface Science, 15*(5), 365–373.

Wu, G., Bazer, F. W., & Cross, H. R. (2014). Land-based production of animal protein: Impacts, efficiency, and sustainability. *Annals of the New York Academy of Sciences, 1328*(1), 18–28.

Xu, T., Yang, J., Hua, S., Hong, Y., Gu, Z., Cheng, L., et al. (2020). Characteristics of starch-based Pickering emulsions from the interface perspective. *Trends in Food Science & Technology, 105*, 334–346.

Yang, J., de Wit, A., Diedericks, C. F., Venema, P., van der Linden, E., & Sagis, L. M. C. (2022). Foaming and emulsifying properties of extensively and mildly extracted Bambara groundnut proteins: A comparison of legumin, vicilin and albumin protein. *Food Hydrocolloids, 123*, Article 107190.

Yang, J., Kornet, R., Diedericks, C. F., Yang, Q., Berton-Carabin, C. C., Nikiforidis, C. V., et al. (2022). Rethinking plant protein extraction: Albumin—from side stream to an excellent foaming ingredient. *Food Structure, 31*, Article 100254.

Yang, J., Thielen, I., Berton-Carabin, C. C., van der Linden, E., & Sagis, L. M. C. (2020). Nonlinear interfacial rheology and atomic force microscopy of air-water interfaces

stabilized by whey protein beads and their constituents. *Food Hydrocolloids, 101*, Article 105466.
Yang, J., Waardenburg, L. C., Berton-Carabin, C. C., Nikiforidis, C. V., van der Linden, E., & Sagis, L. M. C. (2021). Air-water interfacial behaviour of whey protein and rapeseed oleosome mixtures. *Journal of Colloid and Interface Science, 602*, 207–221.
Ye, J., Shi, N., Rozi, P., Kong, L., Zhou, J., & Yang, H. (2024). A comparative study of the structural and functional properties of chickpea albumin and globulin protein fractions. *Food and Bioprocess Technology*.